Veterinary Integrative Sciences 2025; 23(3): e2025065-1-30. DOI: 10.12982/VIS.2025.065

Faculty of Veterinary Medicine
Chiang Mai University

Veterinary Integrative Sciences
ISSN: 2629-9968 (online)

Research article

Computational multi-epitope based design of a multivalent subunit vaccine against co-infecting African swine fever virus and porcine circovirus type 2

Lauren Emily Fajardo[1], Edward C. Banico[1], Ella Mae Joy S. Sira[1], Nyzar Mabeth O. Odchimar[1] and Fredmoore L. Orosco[1, 2, 3, *]

[1]Virology and Vaccine Research Program, Department of Science and Technology—Industrial Technology Development Institute, Taguig, Metro Manila 1631, Philippines
[2]S&T Fellows Program, Department of Science and Technology, Taguig, Metro Manila 1631, Philippines
[3]Department of Biology, College of Arts and Sciences, University of the Philippines Manila, Manila, Metro Manila 1000, Philippines

Abstract

African swine fever virus (ASFV) and porcine circovirus type 2 (PCV2) are two prevalent and economically significant viruses causing high rates of pig mortality and large-scale losses to global pork production. Since there is currently no vaccine simultaneously targeting both viruses, this study aimed to computationally design a safe, stable, and effective multi-epitope based multivalent subunit vaccine against co-infecting ASFV and PCV2. Cytotoxic T-lymphocyte (CTL), helper T-lymphocyte (HTL), and linear B-lymphocyte (LBL) epitopes were screened from sequences of the Rep, Cap, and ORF3 PCV2 proteins. PCV2 epitopes predicted to be antigenic, non-allergenic, and non-toxic were linked to previously screened ASFV epitopes and *Vibrio vulnificus* FlaB flagellin as an adjuvant to create the final vaccine construct, which underwent physicochemical assessment and structure prediction. The vaccine construct was predicted to be stable, soluble, non-cross-reactive, antigenic, and nonallergenic. An immune simulation demonstrated that the vaccine could elicit robust antibody, T-cell, and B-cell responses. The vaccine construct stably docked to TLR5 and formed significant molecular interactions. A 200-ns molecular dynamics simulation showed that the vaccine-TLR5 complex exhibited stability and compactness throughout the run. These results show that the designed vaccine is safe, stable, and effective and warrants experimental validation.

Keywords: African Swine Fever Virus (ASFV), Epitope, Immunoinformatics, Porcine Circovirus Type 2 (PCV2), Subunit vaccine.

*Corresponding author: Fredmoore L. Orosco, Virology and Vaccine Research Program, Department of Science and Technology—Industrial Technology Development Institute, Taguig, Metro Manila 1631, Philippines. E-mail: orosco.fredmoore@gmail.com

Article history; *received manuscript: 5 September 2024, revised manuscript: 11 October 2024, accepted manuscript: 21 October 2024, published online: 31 October 2024,*
Academic editor; *Prapas Patchanee*

INTRODUCTION

African swine fever virus (ASFV) is a large, double-stranded DNA virus of the *Asfarviridae* family that is approximately 190-193 kbp in size and contains over 150 open reading frames (ORFs) (Kim et al., 2023). It is the causative agent of African swine fever (ASF), a disease characterized by high fever, loss of appetite, vomiting, and diarrhea. ASF has a mortality rate of nearly 100% in domestic pigs and can lead to death within a few days of infection (Hsu et al., 2023). The virus was first described in Kenya in 1921 and remained endemic to Africa until 1957 when it was first reported in Europe (Arzt et al., 2010). The virus spread to Asia in 2018 (Kim et al., 2023), with the first outbreak in the Philippines reported in July 2019 (Hsu et al., 2023). As of December 2023, 72 of 82 provinces in the Philippines have experienced ASF outbreaks, with active ASF cases in 71 barangays in 28 municipalities of 10 provinces (Food and Agriculture Organization of the United Nations, 2024). It has been reported in 52 countries worldwide, with approximately 8,000 outbreaks in domestic pigs, 19,000 outbreaks in wild boars, and an overall loss of approximately 1,809,000 swine from January 2021 to December 2023 (World Organisation for Animal Health, 2024). Other swine viruses have been found to co-infect with ASFV, including porcine circovirus type 2 (PCV2). Co-infection of ASFV and PCV2 was first reported in 2021 (Dundon et al., 2022) in Indonesia and Mongolia, and has since been reported in Nigeria (Luka et al., 2022), China (Liu et al., 2023), and Northeast India (Buragohain et al., 2023). PCV2 has been found to enhance the infection and replication of other pathogens (Ouyang et al., 2019) and may exacerbate the effects of ASFV as well.

PCV2 is an emerging swine virus that causes post-weaning multi-systemic wasting syndrome (PMWS) in pigs, more commonly known as porcine circovirus-associated disease (PCVAD) in North America and porcine circovirus disease (PCVD) in Europe. PCVAD mainly manifests in piglets, and its clinical signs may include weight loss, enlarged lymph nodes, respiratory distress, diarrhea, and jaundice (Meng, 2013). PCV2 was first detected in the Philippines in 2004 in Northern Luzon based on the characteristic lymphoid lesions of PCVAD found during post-mortem and histopathological examination, which were verified to contain PCV2 DNA (Maldonado et al., 2004). A recent survey of piggeries in Bulacan and Pampanga found that PCV2 and PCVAD continue to persist in some provinces in the Philippines (dela Cruz et al., 2021).

PCV2 is a member of the *Circoviridae* family and the smallest known virus that infects mammals. It is a single-stranded circular DNA virus approximately 1.7 kB in size, encoding a limited number of proteins. It has approximately 10 open reading frames (ORFs), and three of these ORFs are well-characterized and well-documented. ORF1 encodes the replicase protein, ORF2 encodes the capsid protein Cap, and ORF3 encodes an unnamed protein involved in the cell division cycle of the host cell that can induce cell-mediated apoptosis, and can also contribute to viral pathogenesis in vitro and in vivo (Guo et al., 2022). There are nine known PCV2 genotypes, PCV2a to PCV2i (Chen et al., 2023), with PCV2a, PCV2b, and PCV2d being the most prevalent genotypes.

With the widespread availability of genomic data from countless organisms and the increase in the computational power of bioinformatics tools, reverse vaccinology has become a popular method for designing vaccines against various pathogens. Reverse vaccinology uses genomic data to identify potential antigens against a pathogen of interest. The peptide sequences of these antigens or their epitopes can be linked to form a subunit vaccine, often with an adjuvant that increases the immunogenicity of the vaccine (Clark and Pazdernik, 2016; Orosco and Espiritu, 2024).

There are two live attenuated vaccines against ASFV approved for use in Vietnam (Lu et al., 2023), while there are five globally commercially available vaccines against PCV2, categorized as either inactivated or subunit vaccines and

mainly designed based on the Cap protein. However, live attenuated vaccines may revert to their wild-type form or mutate into a new pathogenic strain, and both live attenuated vaccines and inactivated vaccines are characterized by slow and costly production (Yadav et al., 2020). Furthermore, most PCV2 vaccines were developed to protect against PCV2a, but as the dominant genotype shifted from PCV2a to PCV2b and PCV2d, there are concerns that current vaccines cannot provide sufficient cross-protection (Guo et al., 2022). Subunit vaccines designed based on the current dominant genotypes of ASFV and PCV2 can overcome the aforementioned problems.

Co-infection of ASFV and PCV2 could potentially lead to significantly more detrimental effects than those caused by the individual viruses. Therefore, this study aimed to computationally design a multivalent, multi-epitope subunit vaccine against co-infecting ASFV and PCV2 using epitopes derived from conserved regions of ASFV and PCV2 proteins from dominant genotypes, along with an adjuvant, and connected by appropriate linkers. The study also aimed to evaluate the quality of the vaccine construct at the secondary and tertiary structure levels and to assess its ability to induce an immune response through immune simulation experiments, as well as its binding capability and stability through molecular docking and molecular dynamics experiments. This is the first study to design a multi-epitope multivalent subunit vaccine against ASFV and PCV2.

MATERIALS AND METHODS

Protein retrieval and variability masking

Reference sequences of the Rep (GenBank accession no. YP_010774699.1), Cap (GenBank accession no. YP_010774700.1), and ORF3 (GenBank accession no. YP_006355434.1) proteins of PCV2 were retrieved from the National Center for Biotechnology Information (NCBI) GenBank (ncbi.nlm.nih.gov) (Sayers et al., 2022). Up to 400 sequences for each protein were retrieved using BLASTp (blast.ncbi.nlm.nih.gov/Blast.cgi?PAGE=Proteins) (Altschul et al., 1990) and aligned using ClustalW in MEGA11 (Tamura et al., 2021). Highly conserved fragments with a Shannon entropy (H) of ≤1.0 were identified using the Protein Variability Server (imed.med.ucm.es/PVS) (Díez-Rivero and Reche, 2009) and kept for epitope prediction.

LBL epitope prediction

Linear B-lymphocyte (LBL) epitopes were predicted using BepiPred 3.0 (services.healthtech.dtu.dk/services/BepiPred-3.0) (Clifford et al., 2022), SVMTrip (sysbio.unl.edu/SVMTriP) (Yao et al., 2012), ABCpred (webs.iiitd.edu.in/raghava/abcpred) (Saha and Raghava, 2006; Saha and Raghava, 2007), and LBtope (webs.iiitd.edu.in/raghava/lbtope) (Singh et al., 2015; Singh et al., 2013) with default parameters. A peptide that was (1) recognized as an epitope by BepiPred, (2) recognized as an epitope by either SVMTrip or ABCPred, and (3) recognized as an epitope by LBtope with ≥60% probability; and (4) ≥6 amino acids in length was considered an LBL epitope.

CTL epitope prediction

Cytotoxic T-lymphocyte (CTL) epitopes were first screened for major histocompatibility complex (MHC)-I binding prediction against 45 swine leukocyte antigens (SLAs) in NetMHCCons 1.1 (services.healthtech.dtu.dk/services/NetMHCcons-1.1) (Karosiene et al., 2012). These SLAs are commonly used receptors to predict of CTL epitopes for swine vaccines (Ros-Lucas et al., 2020; Buan et al., 2022; Juan et al., 2022; Simbulan et al., 2024). Peptides that were 9 amino acids long and had a percentile rank of ≤0.5 were considered strong

binders and kept for further analysis. Promiscuous epitopes, i.e. epitopes that strongly bind to 20% of MHC molecules, were prioritized. MHC-I processing prediction was conducted to further screen candidate epitopes in NetCTLpan 1.1 (services.healthtech.dtu.dk/services/NetCTLpan-1.1) (Stranzl et al., 2010) using the default parameters of the server. Peptides with a percentile rank of ≤0.5 were considered CTL epitopes.

HTL epitope prediction

Helper T-lymphocyte (HTL) epitopes were screened for MHC-II binding and processing prediction against 21 human leukocyte antigens (HLAs) in NetMHCIIpan 4.1 (services.healthtech.dtu.dk/services/NetMHCIIpan-4.1) (Reynisson et al., 2020) as MHC-II binding and processing prediction against SLAs was not available on the server. Peptides that were 15 amino acids long and had a percentile rank of ≤10 were considered HTL epitopes. Promiscuous epitopes were prioritized, similar to CTL epitopes.

Epitope antigenicity, allergenicity, toxicity, immunogenicity, and IL-10-inducing potential prediction

Epitopes that had an antigenicity score of ≥0.4 in Vaxijen 2.0 (ddg-pharmfac.net/vaxijen/VaxiJen/VaxiJen.html) (Doytchinova and Flower, 2007) were non-allergenic in AllerTOP 2.0 (ddg-pharmfac.net/AllerTOP), (Dimitrov et al., 2013) were non-toxic in ToxinPred (webs.iiitd.edu.in/raghava/toxinpred) (Gupta et al., 2013), had an immunogenicity score of >0.25 in the Immune Epitope Database (IEDB) Class I immunogenicity prediction server (tools.iedb.org/immunogenicity) (Calis et al., 2013) for CTL epitopes, or had a combined score of <50 in the IEDB CD4 T-cell immunogenicity prediction server (tools.iedb.org/CD4episcore) (Dhanda et al., 2018) and were non-IL-10 inducing as predicted by IL-10Pred (webs.iiitd.edu.in/raghava/il10pred) (Nagpal et al., 2017) for HTL epitopes, were selected as the final epitopes for the vaccine construct.

Vaccine construction and evaluation

PCV2 epitopes were joined to previously screened ASFV epitopes from the same research group (Simbulan et al., 2024) in the following order from the N- to C-terminal: PCV2 LBL – ASFV LBL – PCV2 CTL – ASFV CTL – PCV2 HTL – ASFV HTL. LBL, CTL, and HTL epitopes were joined using KK, AAY, and GPGPG linkers, respectively (Maleki et al., 2022). The HEYGAEALERAG linker was used to join epitopes of different types (Tarrahimofrad et al., 2021). A 6x His-tag was connected to the last epitope (Maleki et al., 2022). The linked epitopes were separately joined to eight different adjuvants at the N-terminus using the EAAAK linker (Pang et al., 2022): *Sus scrofa* β-defensin-1 (*β*d1) (Fagbohun et al., 2022), F3-A6 ASFV hemagglutinin peptides (Buan et al., 2022), phenol-soluble modulin α4 (PSMα4) (Pang et al., 2022), 50S ribosomal protein L7/L12 (Maleki et al., 2022), heparin-binding hemagglutinin adhesin (HBHA) (Lei et al., 2020), *Mycobacterium tuberculosis* heat shock protein 70 (Hsp70) (Lu et al., 2021), *Vibrio vulnificus* flagellin B (FlaB) (Lu et al., 2021), and *Pseudomonas aeruginosa* major outer membrane lipoprotein I (Oprl) (Zhang et al., 2023).

Vaccine constructs with an antigenicity score of ≥0.4 in Vaxijen 2.0, were non-allergenic in AllerTOP, had no homology (<80% sequence similarity) to proteins of *Sus scrofa, S. scrofa domestica,* and *S. scrofa domesticus* in BLASTp, were soluble upon overexpression in *Escherichia coli* in SCRATCH SolPro (scratch.proteomics.ics.uci.edu) (Magnan et al., 2009), and were stable (instability index <40) in Expasy Protparam (web.expasy.org/protparam) (Gasteiger et al., 2005) were retained for further analysis. The physicochemical properties of the vaccine construct, such as molecular weight, isoelectric point (pI), instability index,

aliphatic index, grand average of hydropathy (GRAVY) score, extinction coefficient at 280 nm, and estimated half-life in mammalian reticulocytes, yeast, and *E. coli* were also evaluated in Expasy Protparam.

Secondary and tertiary structure prediction

The secondary structure was predicted using GOR4 (npsa-prabi.ibcp.fr/cgi-bin/npsa_automat.pl?page=/NPSA/npsa_gor4.html) (Garnier et al., 1996) while globular and disordered regions were predicted using GlobPlot 2.3 (globplot.embl.de) (Linding et al., 2003). The tertiary structure was predicted in ColabFold 1.5.2 using AlphaFold2 (colab.research.google.com/github /sokrypton/ColabFold/blob/main/batch/AlphaFold2_batch.ipynb) (Jumper et al., 2021; Mirdita et al., 2022). The top-ranking structure was refined in GalaxyRefine (galaxy.seoklab.org/cgi-bin/submit.cgi?type=REFINE) (Heo et al., 2013). The refined structure with the lowest MolProbity value was selected for further analysis. The local model quality and overall model quality of the predicted structure were validated using the Protein Structural Analysis (ProSA) web server (Sippl, 1993; Wiederstein and Sippl, 2007), and the ERRAT score and Rama-favored regions were assessed using the SAVES 6.0 (saves.mbi.ucla.edu) ERRAT and PROCHECK modules, respectively (Colovos and Yeates, 1993; Laskowski et al., 1993). Conformational B-lymphocyte epitopes were predicted using the IEDB Discotope 1.1 server (tools.iedb.org/discotope) (Haste Andersen et al., 2006).

Immune simulation

The host immune response upon administration of the vaccine was predicted using C-Immsim (kraken.iac.rm.cnr.it/C-IMMSIM) (Rapin et al., 2010) using the parameters of Buan et al. (2022). Two injections of 1000 vaccine particles were administered at time steps 1 and 63, and the entire simulation was run for 100 time steps. The vaccine with ASFV epitopes only, the vaccine with PCV2 epitopes only, and the adjuvant alone were used as controls and were simulated using the same parameters.

Molecular docking of CTL epitopes to SLA-1*04:01

The PCV2 CTL epitopes used in the final vaccine construct were docked to a swine MHC-I molecule, SLA-1*04:01, in GalaxyPepDock (galaxy.seoklab.org/cgi-bin/submit.cgi?type=PEPDOCK (Lee et al., 2015)). The experimentally-determined structure of SLA-1*04:01 (PDB ID: 3QQ3) (Zhang et al., 2011a; Zhang et al., 2011b) was retrieved from the Research Collaboratory for Structural Bioinformatics Protein Data Bank (RCSB PDB) (Berman et al., 2000) and cleaned of ligands and water molecules using PyMOL 2.5.5 (pymol.org/2) (Schrödinger, 2023). An influenza-derived epitope (NSDTVGWSW) was removed from the structure and used as a positive control alongside an ebola-derived epitope (ATAAATEAY) bound to SLA-1*04:01 in a separate structure (PDB ID: 3QQ4) (Zhang et al., 2011a; Zhang et al., 2011c).

Molecular docking of vaccine construct to TLR5

The entire vaccine construct was docked to human toll-like receptor 5 (TLR5) (PDB ID: 3J0A) (Modis et al., 2011; Zhou et al., 2012) in ClusPro 2.0 (cluspro.bu.edu) (Kozakov et al., 2013; Kozakov et al., 2017; Vajda et al., 2017; Desta et al., 2020). The TLR5 structure was cleaned using PyMOL 2.5.5 and missing residues were filled using Modeller (salilab.org/modeller) (Šali and Blundell, 1993). The *Salmonella typhimurium* flagellin FliC (PDB ID: 3A5X) (Maki-Yonekura et al., 2009; Maki-Yonekura et al., 2010), a known TLR5 agonist previously used as a ligand for molecular docking to TLR5 (Savar and Bouzari, 2014) and in recombinant virus-like particles (VLPs) against PCV2 (Liu et al., 2020), was used as a positive control. Binding free energies (ΔG) were calculated using PRODIGY on the EOSC-WeNMR portal (wenmr.science.uu.nl/prodigy) (Vangone and Bonvin, 2015; Xue et al., 2016;

Honorato et al., 2021) and molecular interactions were predicted using PDBSum (www.ebi.ac.uk/thornton-srv/databases/pdbsum) (Laskowski et al., 2018).

Molecular dynamics

Molecular dynamics simulations of the vaccine construct docked to TLR5 were performed in GROMACS 2023.2 (gromacs.org) (Abraham et al., 2015) using the CHARMM36-AA force field and TIP3P water model. Sodium and chloride counter ions were added to neutralize the system. Energy minimization was performed in 50000 steps using the steepest descent algorithm. The system was equilibrated at a temperature of 300 K and a pressure of 1 bar using the Berendsen thermostat at a time step of 2 fs. The production simulation was run for 200 ns for the calculation of the root mean square deviation (RMSD), the root mean square fluctuation (RMSF), the radius of gyration (Rg), the number of hydrogen bonds, and the solvent-accessible surface area (SASA).

RESULTS

Protein retrieval and variability masking

A total of 400 sequences for Cap, 400 sequences for Rep, and 155 sequences for ORF3 were retrieved from NCBI. The Protein Variability Server revealed that 99.57% of residues were conserved in Cap, 99.36% of residues were conserved in Rep, and 98.04% of residues were conserved in ORF3. Variable residues were removed and contiguous conserved peptides were retained for epitope prediction.

LBL epitope prediction

From the conserved fragments of the PCV2 protein sequences, five (5) peptides were predicted as LBL epitopes by BepiPred 3.0, SVMTrip, ABCpred, and LBtope, four (4) of these epitopes had an antigenicity score of >0.4 in VaxiJen 2.0, and only two (2) epitopes were both non-allergenic in AllerTOP 2.0, and non-toxic in ToxinPred. Both epitopes were included in the final vaccine construct and are listed in Table 1 along with their antigenicity scores.

Table 1 Antigenicity scores of the final LBL epitopes predicted from PCV2 protein sequences.

LBL epitopes	Antigenicity scores
HVGLGTAFENSIYDQE	0.8550
NGHQTPALQQGTHSSR	0.5694

LBL, linear B-lymphocyte.

CTL epitope prediction

Of the 580 9-mer peptides as potential CTL epitopes, 55 were strongly binding (PR <0.5) to MHC-I in NetMHCCons 1.1, 24 were predicted as epitopes (PR <1.0) in NetCTLpan 1.1, 17 of these epitopes had an antigenicity score of >0.4, 11 epitopes were both non-allergenic and non-toxic, and seven (7) epitopes had an immunogenicity score of >0 in the IEDB CD4 T-cell immunogenicity prediction server. Among these epitopes, the five (5) epitopes with the highest antigenicity scores were included in the final vaccine construct and are listed in Table 2 along with their corresponding scores.

Table 2 Antigenicity, antigen processing, and antigen presentation scores of the final CTL epitopes predicted from PCV2 protein sequences.

CTL epitopes	Antigenicity scores	No. of strong binding MHC-I	Cleavage scores	TAP scores	Immunogenicity scores
MTYPRRRYR	1.0603	2	0.49293	1.914	0.12828
ATALTYDPY	1.0375	8	0.79483	3.25	0.0481
KRNQLWLRL	0.8304	1	0.96821	1.238	0.09993
RWFPVCGFR	0.7556	2	0.63723	2.076	0.11329
YRRITSLVF	0.5899	1	0.97127	2.798	0.04755

CTL, cytotoxic T-lymphocyte; MHC-I, major histocompatibility complex I, TAP, transporter associated with antigen processing.

HTL epitope prediction

Among the 535 15-mer peptides as potential HTL epitopes, 348 peptides were predicted to be epitopes with strong binding to MHC-II molecules (PR ≤10%) in NetMHCIIpan 4.1, 205 epitopes had an antigenicity score of >0.4, 129 epitopes were both non-allergenic and non-toxic, and 29 epitopes had a combined score of <50 in the IEDB Class I immunogenicity prediction server, and 18 epitopes were non-IL-10 inducing. Among these epitopes, the five (5) epitopes with the highest antigenicity scores were included in the final vaccine construct and are listed in Table 3 along with their corresponding scores.

All LBL, CTL, and HTL epitopes included in the final vaccine construct surpassed the antigenicity threshold of 0.4 for viruses in VaxiJen 2.0, were determined to be non-allergenic in AllerTOP 2.0, and were determined to be non-toxic in ToxinPred. A summary of the epitopes used in vaccine constructs is presented in Table 4.

Table 3 Antigenicity, antigen presentation, and cytokine-inducing potential scores of the final HTL epitopes predicted from the PCV2 protein sequences.

HTL epitopes	Antigenicity scores	No. of strong binding MHC-II	Immunogenicity scores	IL-10 inducer
SIYDQEYNIRVTMYV	0.9649	1	49.04292	No
HRYRWRRKNGIFNTR	0.8229	2	45.52692	No
VPFEYYRIRKVKVEF	0.7168	10	43.7794	No
TPLEWYSSTAVPAVE	0.6408	18	47.63588	No
RNQLWLRLQTAGNVD	0.6302	5	45.80012	No

HTL, helper T-lymphocyte; MHC-II, major histocompatibility complex II; IL-10, interleukin-10.

Vaccine construction and evaluation

All eight adjuvant candidates in this study have been previously used in both in silico and in vitro vaccine design studies. For instance, F3-A6, Hsp70, FlaB, and OprI have been used as adjuvants in ASFV vaccines. Among the adjuvant candidates, four (L7/L12, Hsp70, FlaB, and OprI) produced vaccine constructs that were antigenic, non-allergenic, soluble, stable, and showed zero cross-reactivity with swine proteins. However, following tertiary structure prediction and refinement, only the FlaB-adjuvanted vaccine construct achieved an ERRAT score ≥95%. Therefore, it was used for the final vaccine construct. The complete results of the evaluation of adjuvant candidates can be found in Table 5. The FlaB adjuvant was joined to the epitopes at the N-terminus of the vaccine construct using an EAAAK linker. The LBL, CTL, and HTL epitopes were joined by KK, AAY, and GPGPG linkers, respectively. The HEYGAEALERAG linker was used to join different epitope groups. A 6x His-tag was added to the C-terminus of the vaccine construct. Figure 1 depicts graphical (Figure 1A) and cartoon (Figure 1B) representations of the final vaccine constructs.

Table 4 Final epitope components of the ASFV+PCV2 multi-epitope subunit vaccine construct.

Virus	Groups	Epitopes	Source proteins (ORFs)

ASFV	LBL	GIAGRGIPLGNPHVKP	Minor capsid protein (B438L)
		LDAVKMDKRNIK	Envelope protein p22 (KP177R)
		AKLQDTKFKWKYTLDP	Transmembrane protein (C257L)
		GRPSRRNIRFK	Major capsid protein (B646L)
	CTL	TVSAIELEY	Polyprotein p220 (CP2475L)
		KTRDFFILY	Transmembrane (C62L)
		MMDFERVHY	Cysteine protease (S273R)
		KNLSIIWEY	MGF 360-13L
		KAIELYWVF	MGF 360-18R
		YLYEIEIEY	Guanylyltransferase (NP868R)
	HTL	SRRFRFVSLDAYNMG	Termination factor (Q706L)
		KIGFYSSKSTAHERE	Helicase/primase (F1055L)
		ESVYFAVETIHLKQQ	EP424R
		KYWYAIAVDYDLKDA	MGF 360-11L
PCV2	LBL	HVGLGTAFENSIYDQE	Cap
		NGHQTPALQQGTHSSR	ORF3
	CTL	MTYPRRRYR	Cap
		ATALTYDPY	Cap
		KRNQLWLRL	Cap
		RWFPVCGFR	ORF3
		YRRITSLVF	Rep
	HTL	SIYDQEYNIRVTMYV	Cap
		HRYRWRRKNGIFNTR	Cap
		VPFEYYRIRKVKVEF	Cap
		KNGIFNTRLSRTFGY	Cap
		TPLEWYSSTAVPAVE	Rep

ASFV, African swine fever virus; PCV2, porcine circovirus type 2; LBL, linear B-lymphocyte; CTL, cytotoxic T-lymphocyte; HTL, helper T-lymphocyte; ORF, open reading frame; MGF, multigene family.

Table 5 Physicochemical property evaluation of the ASFV+PCV2 vaccine construct with each adjuvant candidate.

Adjuvant	Antigenicity	Allergenicity	Cross-reactivity	Solubility	Stability
βd1	0.8001	Non-allergenic	*Sus scrofa* β-defensin (100% identity)	Soluble (81% probability)	Unstable (41.73)
F3-A6	0.7390	Non-allergenic	None	Soluble (62% probability)	Unstable (43.20)
PSMα4	0.7288	Non-allergenic	None	Soluble (56% probability)	Unstable (41.24)
L7/L12	0.6759	Non-allergenic	None	Soluble (93% probability)	Stable (38.14)
HBHA	0.6260	Non-allergenic	None	Soluble (94% probability)	Unstable (42.66)
Hsp70	0.6677	Non-allergenic	None	Soluble (91% probability)	Stable (37.79)
FlaB	0.7085	Non-allergenic	None	Soluble (80% probability)	Stable (35.13)
OprI	0.7331	Non-allergenic	None	Soluble (70% probability)	Stable (39.48)

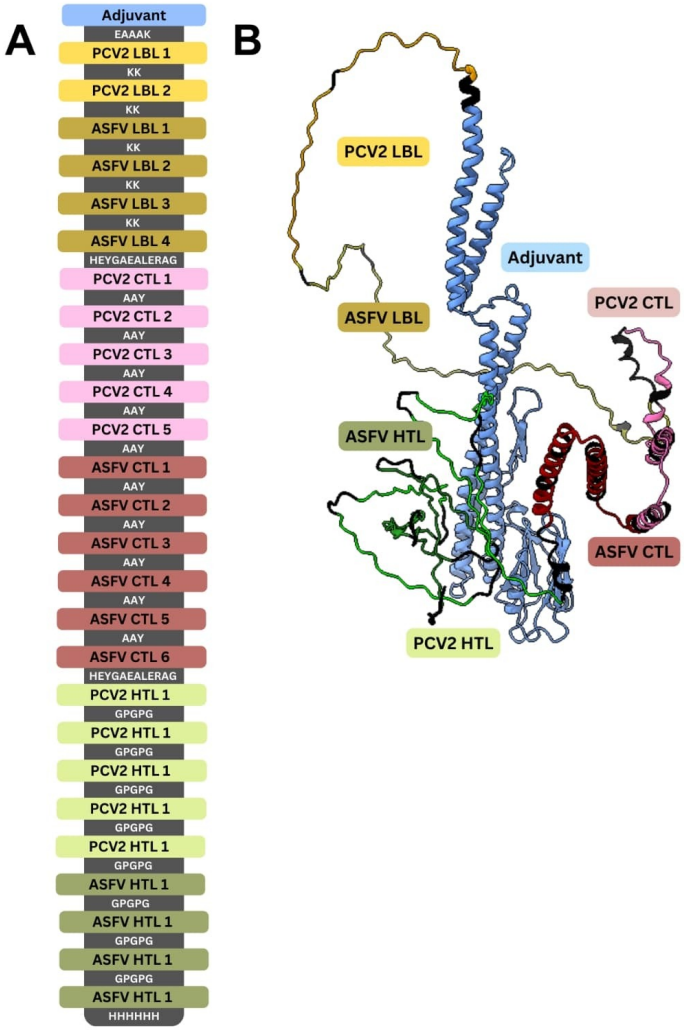

Figure 1 Designed multi-epitope subunit vaccine against co-infecting ASFV and PCV2. (A) Graphical representation of the components of the vaccine construct. (B) Cartoon representation of the predicted tertiary structure of the vaccine construct. ASFV, African swine fever virus; PCV2, porcine circovirus type 2; LBL, linear B-lymphocyte; CTL, cytotoxic T-lymphocyte; HTL, helper T-lymphocyte.

Physicochemical properties

The physicochemical properties of the final FlaB-adjuvanted vaccine constructs are shown in Table 6. It has a molecular weight of approximately 90 kDa, an isoelectric point (pI) of 9.09, an aliphatic index of 73.91, a GRAVY score of -0.532, an extinction coefficient at 280 nm of 122050 m^{-1} cm^{-1}, an estimated half-life of 30 hours in mammalian reticulocytes in vitro, >20 hours in yeast in vivo, and >10 hours in *E. coli* in vivo, and is stable with an instability index of 35.13 (<40) as predicted by Expasy Protparam. It is antigenic with a score of 0.7085, is non-allergenic, has no homology with any swine proteins in NCBI, indicating zero cross-reactivity, and is soluble with 80% probability upon overexpression in *E. coli,* as predicted by SCRATCH SolPro.

Table 6 Physicochemical properties of the final ASFV+PCV2 multi-epitope subunit vaccine construct.

Servers	Properties	Results
Expasy Protparam	Molecular Weight	89937.98 Da
	Isoelectric Point	9.09
	Stability	Stable (Instability Index = 35.13)
	Aliphatic Index	73.91
	GRAVY	Hydrophilic (-0.532)
	Extinction coefficient	122050 m^{-1} cm^{-1}
	Estimated half-life	30 hours (mammalian reticulocytes, in vitro) >20 hours (yeast, in vivo). >10 hours (*E. coli*, in vivo).
VaxiJen 2.0	Antigenicity	Antigenic (0.7085)
AllerTOP 2.0	Allergenicity	Non-allergenic
BlastP	Cross-reactivity	Non-cross-reactive
SolPro	Solubility	Soluble (80% probability)

GRAVY, grand average of hydropathy.

Secondary structure prediction

The secondary structure of the vaccine construct predicted by GOR4 was 46.49% alpha helices, 12.55% extended strands, and 40.96% random coils. GlobPlot 2.3 identified two (2) globular regions: M1-H403 and K448-K660, and eleven (11) disordered regions: V3-T7, F132-T141, Q404-R420, A434-P447, M645-W657, N661-F675, E686-Y698, A702-Q715, T722-R755, D762-S774, and Q786-K793. Some of the predicted disordered regions are within the predicted globular regions. The first globular region spans the entire adjuvant until part of the second PCV2 LBL epitope, whereas the second globular region spans the third ASFV LBL epitope, all CTL epitopes, and up to the second PCV2 HTL epitope. The predicted disordered regions lie within the adjuvant, LBL epitopes, and HTL epitopes. No disordered regions were predicted in the CTL epitopes. The globular and disordered regions were mapped to the tertiary structure of the final vaccine construct (Figure 2).

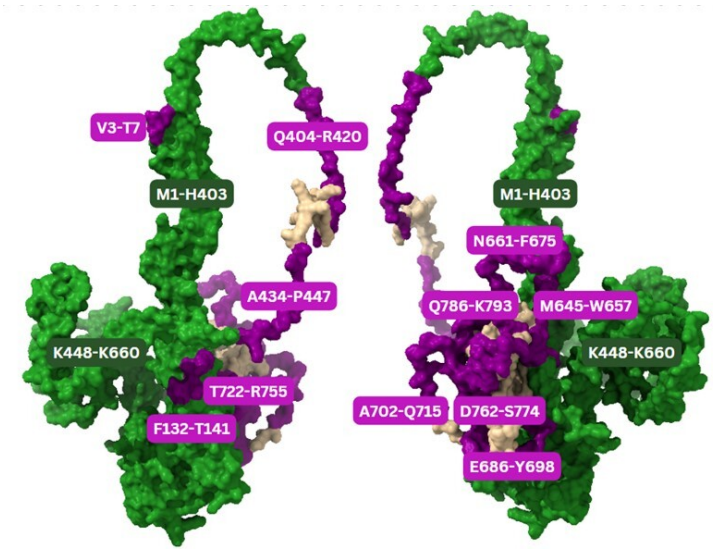

Figure 2 Globular (green) and disordered (regions) mapped to the final ASFV+PCV2 multi-epitope subunit vaccine construct.

Tertiary structure prediction

The tertiary structure of the vaccine construct predicted by AlphaFold2 was refined using GalaxyRefine. Five (5) refined models were generated, and the model with the lowest MolProbity score was chosen for further analysis. The overall model quality (Figure 3A) and local model quality (Figure 3B) of the refined vaccine construct were assessed in ProSA. The refined vaccine construct had a z-score of -4.59 in ProSA and an ERRAT score of 96.404. The Ramachandran plot showed that, among the non-glycine and non-proline residues, 96.5% (683) were in the most favored regions, 2.5% (18) were in additional allowed regions, 0.3% (2) were in generously allowed regions, and 0.7% (5) were in disallowed regions, as predicted by PROCHECK.

Forty-three (43) conformational B-lymphocyte epitopes were predicted throughout the entire vaccine construct using the IEDB Discotope 1.1 server: M1-A2, N6, S23, Q26, M29, S33-S34, S40-K42, V56, E84, N87, N101-S105, S107, G133-G134, T141, N153-G154, D183-W186, A190, F203-Q207, E239-G240, A310, N313, H317, S320-N321, N324-I325, E327-S332, S334-R335, A342-K343, T346, G387-A502, D510-R517, F530, C533, A538, I556-E557, M613-A627, R630-Y678, R681, E686-L716, A723-K740, T742-F756, Y764-S774, H783-W795, and Y802-H813. Conformational B-lymphocyte epitopes were mapped to the tertiary structure of the final vaccine construct as shown in Figure 5.

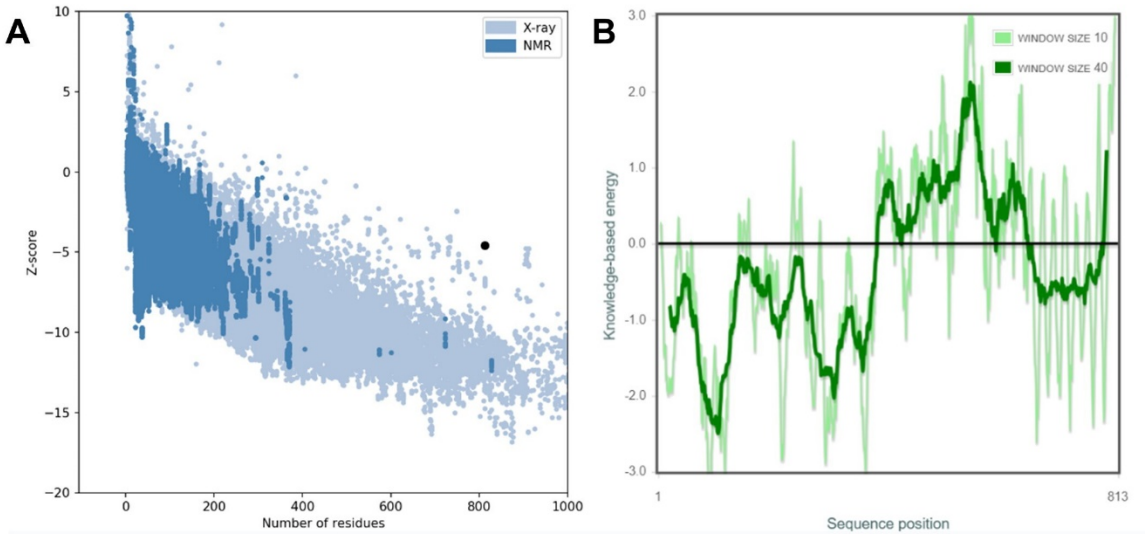

Figure 3 Quality plots of the final ASFV+PCV2 multi-epitope subunit vaccine construct. (A) Overall model quality plot plotting the z-score of the final vaccine construct (black dot) against z-scores of PDB structures experimentally determined by X-ray crystallography (light blue) or nuclear magnetic resonance (NMR) spectroscopy (dark blue). (B) Local model quality plot showing the knowledge-based energy at each position of the final vaccine construct.

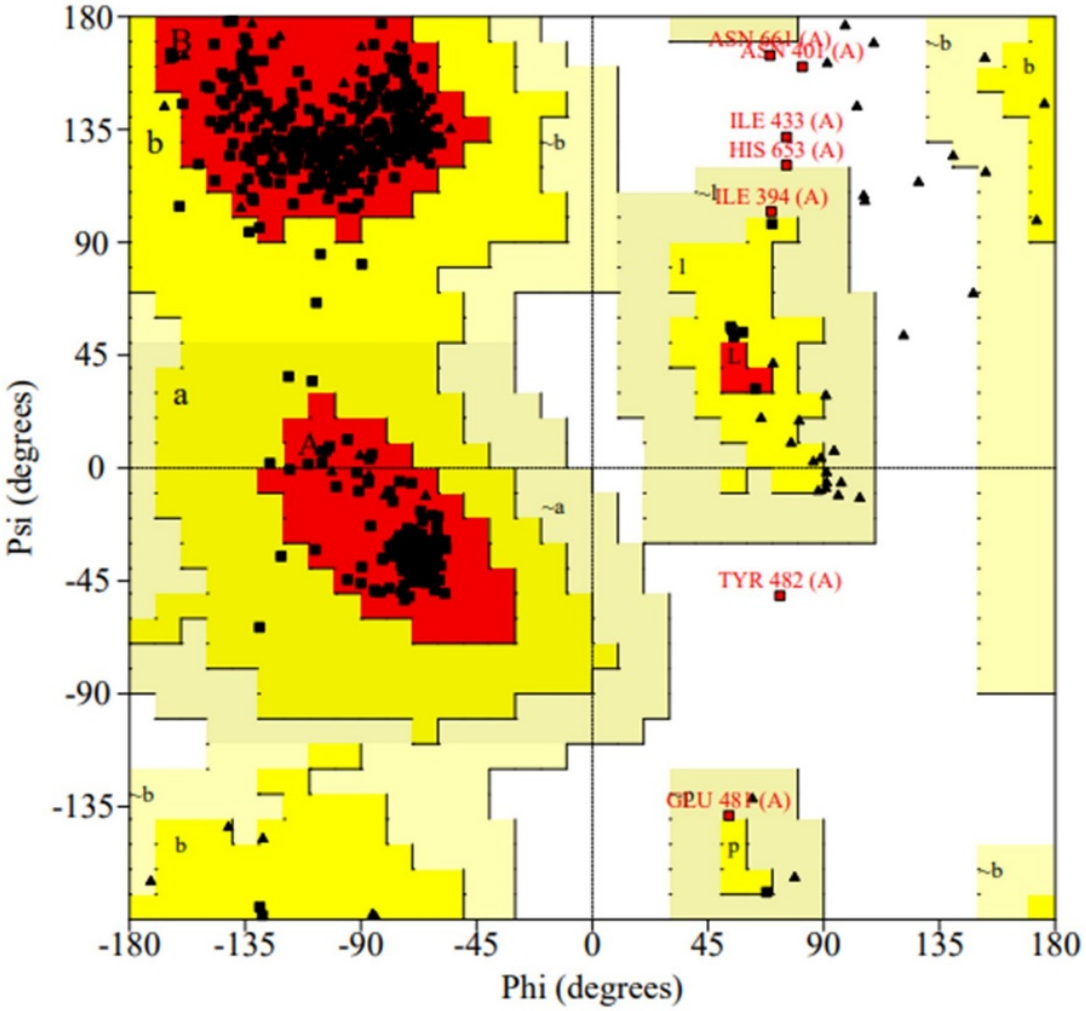

Plot statistics

Residues in most favoured regions [A,B,L]	683	96.5%
Residues in additional allowed regions [a,b,l,p]	18	2.5%
Residues in generously allowed regions [~a,~b,~l,~p]	2	0.3%
Residues in disallowed regions	5	0.7%
Number of non-glycine and non-proline residues	708	100.0%
Number of end-residues (excl. Gly and Pro)	2	
Number of glycine residues (shown as triangles)	74	
Number of proline residues	29	
Total number of residues	813	

Figure 4 Ramachandran plot of the final ASFV+PCV2 multi-epitope subunit vaccine construct.

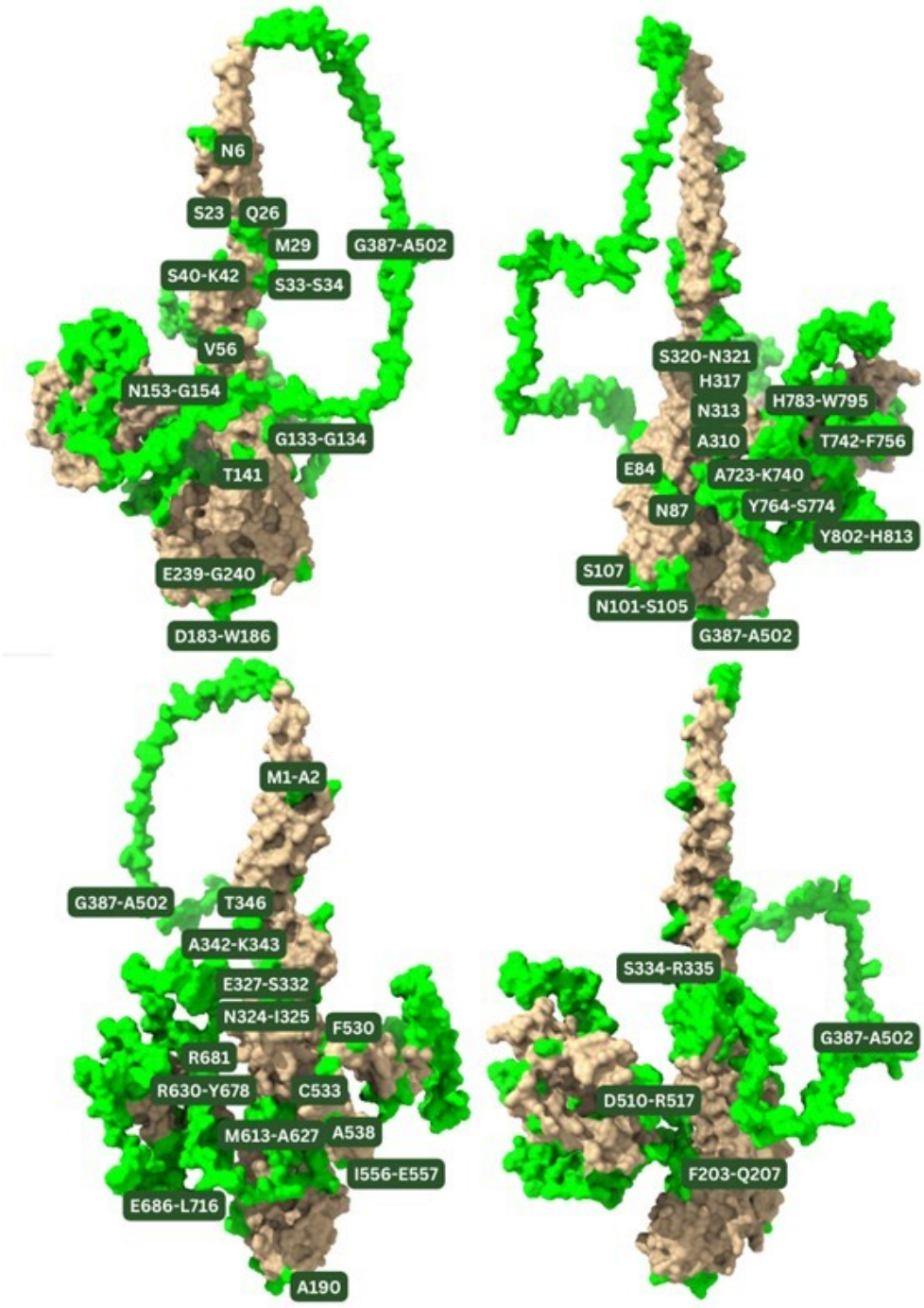

Figure 5 Conformational B-lymphocyte epitopes mapped to the final ASFV+PCV2 multi-epitope subunit vaccine construct.

Immune simulation

Immune simulation using C-ImmSim revealed that the ASFV+PCV2 vaccine construct induced higher antibody titers (Figure 6A) and B-cell population counts (Figure 6B) than the vaccine construct with ASFV epitopes alone, the vaccine construct with PCV2 epitopes alone, the adjuvant alone, and the ASFV vaccine of Buan et al. (Buan et al., 2022) The ASFV+PCV2 vaccine construct and the vaccine construct with PCV2 epitopes alone both had the highest induced T-cell population counts relative to the other groups (Figure 6C).

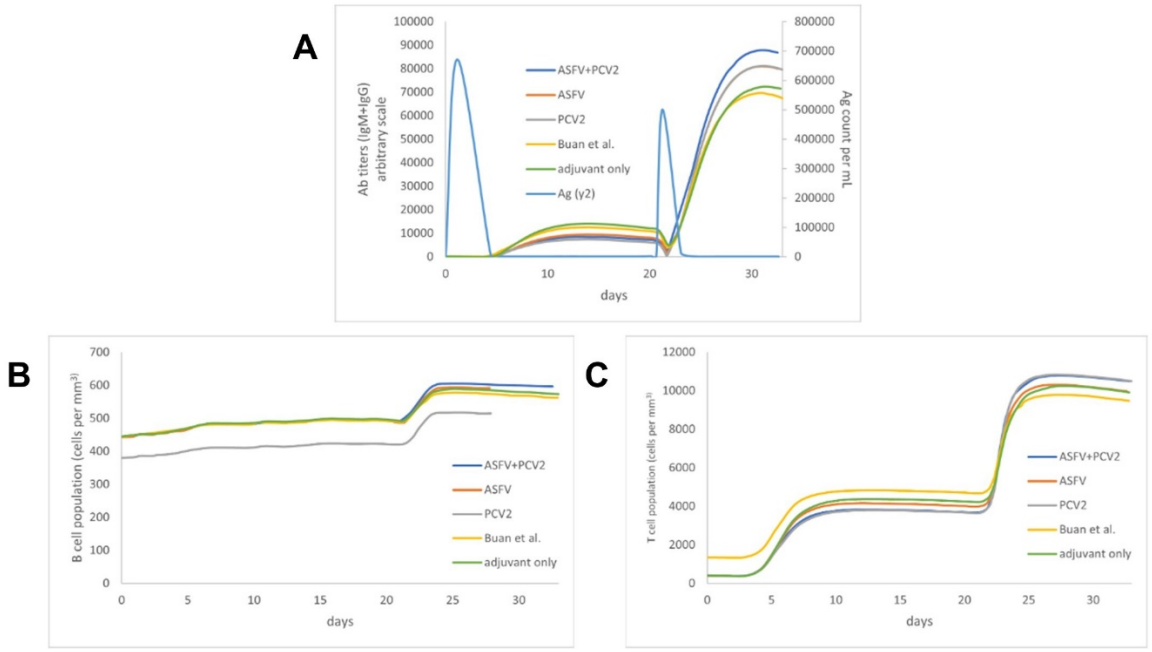

Figure 6 Immune simulation results of the final vaccine construct (blue) compared to the vaccine construct with ASFV epitopes only (orange), the vaccine construct with PCV2 epitopes only (gray), the ASFV vaccine construct of Buan et al., 2022 (yellow), and the FlaB adjuvant alone (green). (A) Antibody titer and antigen count. (B) B-cell population. (C) T-cell population. ASFV, African swine fever virus; PCV2, porcine circovirus type 2.

Molecular docking of CTL epitopes to SLA-1*04:01

The PCV2 CTL epitopes were docked to the swine MHC-I molecule SLA-1*04:01 in GalaxyPepDock, as shown in Figure 7A-E. For the molecular interactions predicted by PDBSum, the number of hydrogen bonds (HB) between the PCV2 CTL epitopes and SLA-1*04:01 ranged from 7 to 11, while the number of non-bonded contacts (NBC) ranged from 85 to 135. This was less than the number of molecular interactions with the influenza-derived epitope (15 HB, 174 NBC) and the Ebola-derived epitope (14 HB, 142 NBC). However, the binding free energies (ΔG) calculated using PRODIGY ranged from -10.7 kcal/mol to -10.0 kcal/mol, similar to the binding free energies of the influenza-derived epitope (-10.8 kcal/mol) and the Ebola-derived epitope (-11.4 kcal/mol), showing strong binding affinity. The results showed that the PCV2 CTL epitopes were successfully docked to and strongly bound to SLA-1*04:01.

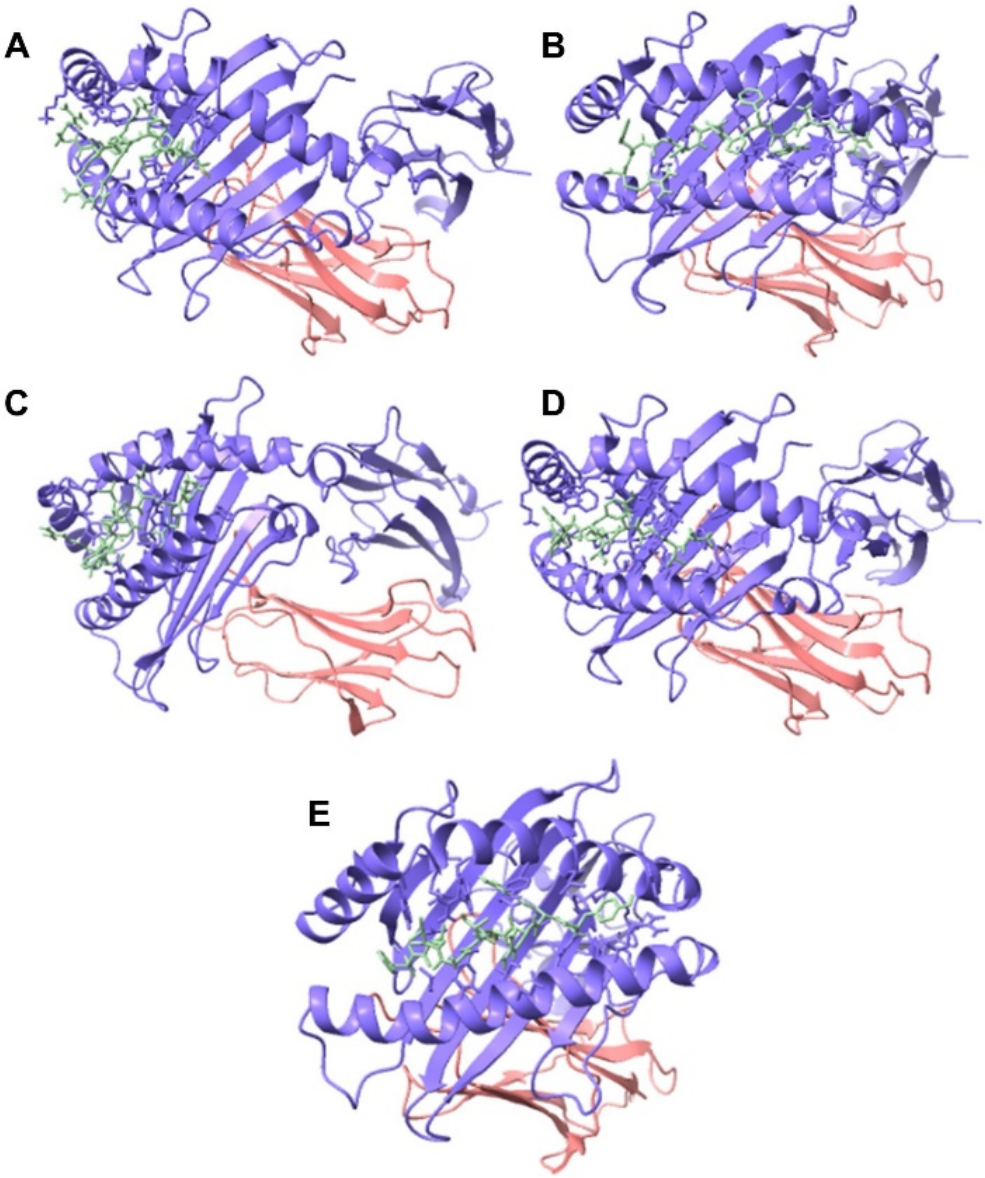

Figure 7 Molecular docking of PCV2 CTL epitopes (green) to SLA-1*04:01 (purple) with β2-microglobulin (pink). (A) MTYPRRRYR, (B) RWFPVCGFR, (C) KRNQLWLRL, (D) ATALTYDPY, (E) YRRITSLVF.

Molecular docking of vaccine construct to TLR5

The entire vaccine construct was also docked to human TLR5 in ClusPro 2.0, as shown in Figure 8, with FliC docked to TLR5 as a positive control. The top-ranked docked model had a center energy score of -1882.4 and the lowest energy score of -2014.1. FliC docked to TLR5 had a center energy score of -975.8 and a lowest energy score of -1118.8. The molecular interactions of the docked complexes were quantified using PDBSum. The vaccine-TLR5 complex formed 10 salt bridges, 41 hydrogen bonds, and 398 non-bonded contacts, while the FliC-TLR5 complex formed 13 hydrogen bonds and 202 non-bonded contacts. No salt bridges were formed in the FliC-TLR5 complex. The binding free energy of the vaccine-TLR5 complex was -18.3 kcal/mol, while the binding free energy of the FliC-TLR5 complex was -16.1 kcal/mol. The energy scores, binding free energies, and number of molecular interactions showed that the vaccine was docked more stably to TLR5 compared to FliC. The negative energy scores, negative binding free

energies, and abundance of molecular interactions demonstrated that the vaccine construct stably docked to TLR5. A summary of the molecular docking results is shown in Table 7.

Table 7 Summary of molecular docking results of PCV2 CTL epitopes to SLA1*04:01 and the final ASFV+PCV2 multi-epitope subunit vaccine construct to TLR5.

Complex	Molecular interactions	ΔG (kcal/mol)
SLA1*04:01-MTYPRRRYR	10 HB, 135 NBC	-10.5
SLA1*04:01-RWFPVCGFR	9 HB, 115 NBC	-10.0
SLA1*04:01-KRNQLWLRL	7 HB, 85 NBC	-10.7
SLA1*04:01-ATALTYDPY	11 HB, 135 NBC	-10.2
SLA1*04:01-YRRITSLVF	11 HB, 112 NBC	-10.3
SLA1*04:01-NSDTVGWSW[1]	15 HB, 174 NBC	-10.8
SLA1*04:01-ATAAATEAY[2]	14 HB, 142 NBC	-11.4
TLR5-ASFV+PCV2 vaccine construct	10 SB, 41 HB, 398 NBC	-18.3
TLR5-*S.* Typhimurium FliC[3]	0 SB, 13 HB, 202 NBC	-16.1

Controls: [1]influenza-derived epitope (PDB ID: 3QQ3), [2]ebola-derived epitope (PDB ID: 3QQ4), [3]known TLR5 agonist (PDB ID: 3A5X). SLA, swine leukocyte antigen; TLR5, toll-like receptor 5; ASFV, African swine fever virus; PCV2, porcine circovirus type 2; HB, hydrogen bonds; NBC, non-bonded contacts.

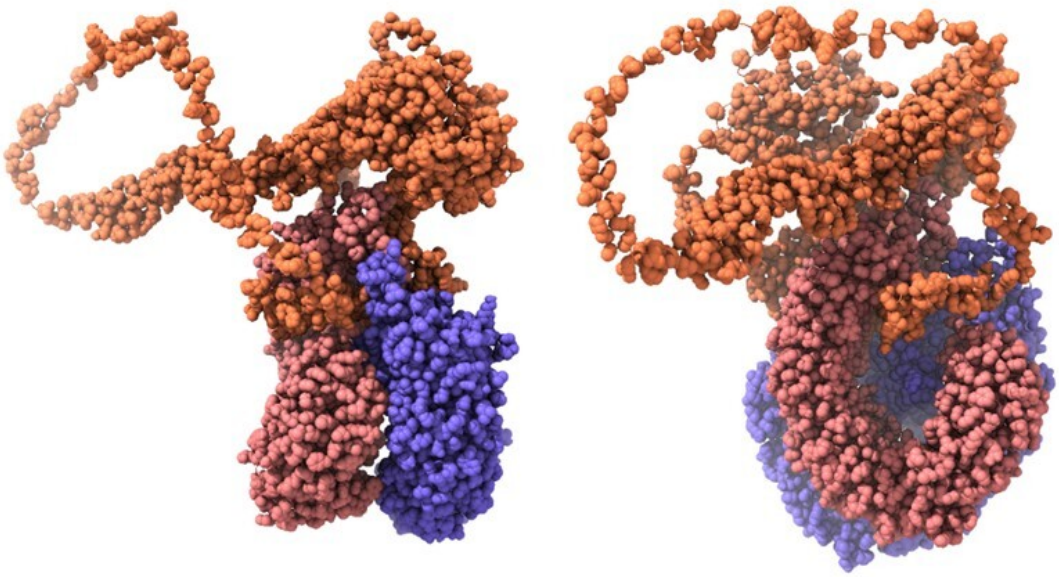

Figure 8 Molecular docking of the final ASFV+PCV2 multi-epitope subunit vaccine construct (orange) to TLR5 (purple and pink).

Molecular dynamics

A 200-ns molecular dynamics simulation was performed for the vaccine-TLR5 complex. The backbone RMSD of the vaccine-TLR5 complex stabilized at approximately 1.8 nm after approximately 60 ns (Figure 9A). The RMSF of the Cα atoms of the vaccine showed an average fluctuation of 0.6916 nm, with the highest fluctuations being at the N- and C-termini as well as the LBL epitopes (Figure 9B). The Rg of the vaccine-TLR5 complex showed a gradual decrease from around 5.6 to 5.1 nm at the 50 ns mark, followed by a gradual increase to approximately 5.3 at approximately 150 ns, and then a sharp drop back to approximately 5.1 nm (Figure 9C). The number of hydrogen bonds formed between the vaccine and TLR5 increased throughout the simulation, from an average of 12 hydrogen bonds from 0 to 100 ns, to an average of 15 hydrogen bonds from 100 to 200 ns (Figure 9D).

The SASA of the complex decreased from approximately 1350 nm^2 to 1150 nm^2 during the simulation (Figure 9E).

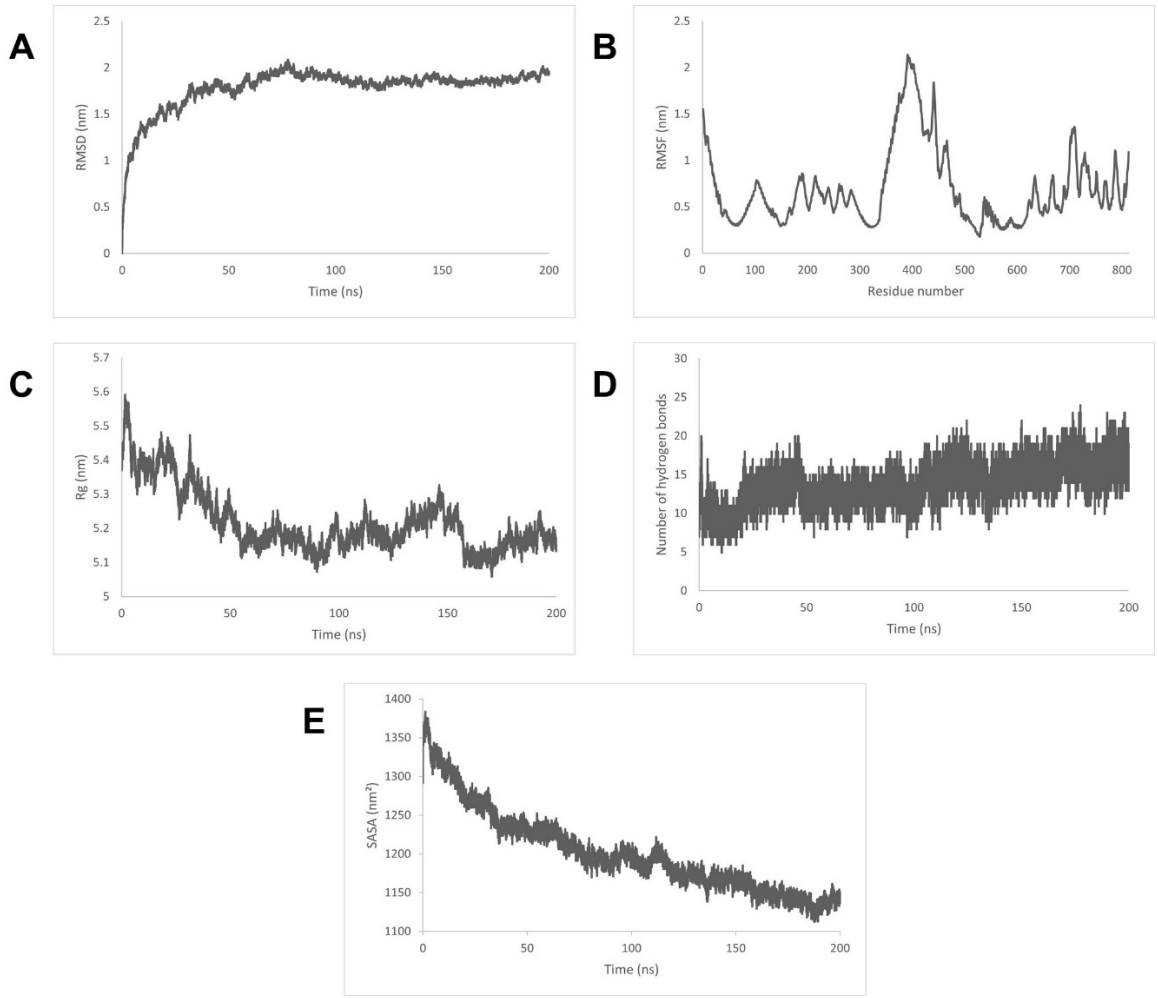

Figure 9 MD simulation analysis of the final ASFV+PCV2 multi-epitope subunit vaccine-TLR5 complex. (A) RMSD of the backbone of the vaccine-TLR5 complex. (B) RMSF of the Cα molecules of the vaccine. (C) Rg of the vaccine-TLR5 complex. (D) Number of hydrogen bonds formed between the vaccine and TLR5. (E) SASA of the vaccine-TLR5 complex.

DISCUSSION

Immunoinformatics has gained immense popularity in recent years for its quick and cost-effective approach in designing vaccines using genomic and proteomic data (Sira et al., 2025). While a number of studies have previously employed in silico approaches in designing epitope-based vaccines against ASFV (Ros-Lucas et al., 2020; Herrera and Bisa, 2021; Buan et al., 2022; Rowaiye et al., 2023), the current study offers a computationally designed multivalent, multi-epitope subunit vaccine against co-infecting ASFV and PCV2, employing a proteomic and genotype-specific approach to screen for epitopes, an assessment of multiple vaccine construct candidates including various known adjuvants, and an extensive evaluation of the quality and stability of the predicted model, supplemented by an atomistic molecular dynamics simulation. Overall, the current study offers a comprehensive analysis using the most advanced tools in reverse vaccinology.

Cap, Rep, and ORF3 protein sequences of PCV2 were retrieved and variability-masked to retain contiguous conserved residues for epitope prediction. The PCV2b and PCV2d genotypes were prioritized in protein retrieval as they are currently the two most dominant PCV2 genotypes worldwide, although representatives from all genotypes available in NCBI were retrieved to predict epitopes that are conserved throughout as many genotypes as possible to provide cross-protection. Likewise, the ASFV epitopes used in the designed vaccine construct and predicted by Simbulan et al. (2024) were sourced from proteins that were selected to prioritize the dominant genotypes I and II.

Two (2) of the predicted LBL epitopes were found to be antigenic, non-allergenic, and non-toxic and were included in the final vaccine construct. B cells are essential for the production of antigen-specific antibodies or immunoglobulins (Igs) that recognize and neutralize pathogens (Althwaiqeb et al., 2023).

Five (5) of the predicted CTL epitopes were found to be antigenic, non-allergenic, non-toxic, and immunogenic and were included in the final vaccine construct. MHC-I molecules are involved in the processing and presentation of antigens to CTLs. In the MHC-I antigen processing pathway, proteins in the cytosol are ubiquitinated and undergo proteasomal degradation to produce short peptides. These peptides are then translocated into the endoplasmic reticulum (ER) by the transporter associated with antigen processing (TAP). TAP recruits other proteins to form the Peptide Loading Complex (PLC), which interacts with the transmembrane glycoprotein tapasin. Tapasin recruits newly synthesized MHC-I molecules and the chaperone calreticulin to the PLC. The peptide binds to MHC-I, then the entire complex is transported from the ER to the Golgi apparatus and finally to the cell surface where it can be recognized by cytotoxic T-lymphocytes (Blum et al., 2013) to elicit immune functions. The IEDB server scores the immunogenicity of peptides based on the observations that positions 4-6 of a peptide are more important for immunogenicity, and that peptides with certain amino acids that are large and/or have aromatic side chains are more immunogenic (Calis et al., 2013). While peptides that bind to MHC-I molecules can be 8-11 residues in length (Zajonc, 2020), only 9-mer peptides were used in this study as NetCTLpan 1.1 and the IEDB server are optimized for 9-mer peptides (Stranzl et al., 2010; Calis et al., 2013). Evaluating binding affinity, proteasomal cleavage, TAP transport efficiency, and immunogenicity are important for selecting CTL epitopes that can induce a robust cytotoxic T-lymphocyte response.

Eighteen (18) of the predicted HTL epitopes were found to be antigenic, non-allergenic, non-toxic, immunogenic, and non-IL-10 inducing. The five (5) HTL epitopes with the highest antigenicity scores were included in the final vaccine construct. MHC-II molecules are involved in the processing and presentation of antigens to HTLs. Unlike in MHC-I antigen processing, peptides do not enter the ER during MHC-II antigen processing. Instead, the MHC-II molecule associates with a chaperone called the invariant chain in the ER; then, the entire complex is directed to the Golgi apparatus and into a late endosome, where the MHC-II molecule is released from the invariant chain to bind to an antigenic peptide. The new complex is then transported to the cell surface where it can be recognized by helper T-lymphocytes (Blum et al., 2013) to elicit immune functions. Immunogenicity was determined by identifying immunogenic motifs 8-11 residues in length within the HTL epitopes, which are generally 15 residues in length (Mishra, 2020). This is based on the number of residues observed to be in contact with the T-cell receptor, and the core binding characteristic of the MHC-II molecule, which is approximately 9 residues long (Dhanda et al., 2018). Helper T-lymphocytes are also predominantly capable of producing cytokines, including IL-10, a potent anti-inflammatory cytokine (Zhang and An, 2007). However, in pigs infected with PCV2, was upregulated in the thymus, leading to thymic depletion and atrophy (Darwich et al., 2003). Darwich et al. (2008) showed that IL-10 was transiently elevated during the peak viremic stage in pigs sub-clinically infected with PCV2. An IL-10 deficient

mice model demonstrated that IL-10 deficiency prevented the depletion of splenic lymphocytes and upregulated cytotoxic T-lymphocyte and helper T-lymphocytes in the lungs through the induction of T-cell chemokines. Simultaneously, PCV2 infection in IL-10 deficient mice led to a significant increase in PCV2-specific antibodies and pro-inflammatory cytokines compared to wild-type mice, resulting in milder lung lesions and lower viral loads (Du et al., 2019). Therefore, only HTL epitopes that were non-IL-10 inducing were incorporated into the final vaccine construct. The selection of strongly binding, immunogenic, and non-IL-10 inducing HTL epitopes is essential for producing a robust helper T-lymphocyte response that is specific to PCV2. However, it must be noted that all ASFV HTL epitopes used in the vaccine construct are IL-10-inducing. As the interaction between co-infecting ASFV and PCV2 within the host is yet to be elucidated, the exact effect of IL-10 induction is unclear and warrants further study.

Unlike alignment-dependent algorithms for antigen identification, which come with many limitations and do not consider the more complex characteristics of proteins, VaxiJen 2.0 uses auto cross covariance (ACC) transformation, a method that converts protein sequences into uniform vectors of equal length that contain information on the physicochemical properties of the amino acids such as hydrophobicity, molecular size, and polarity. The information was compared against a database-derived model of known antigens and known non-antigens to determine antigenicity (Doytchinova and Flower, 2007). All epitopes were determined to be non-allergenic and non-toxic, which is important for ensuring the safety of the vaccine within the host. Similar to VaxiJen 2.0, AllerTOP 2.0 employs auto cross covariance (ACC) transformation to determine allergenicity and uses a k-nearest neighbor algorithm against a dataset of known allergens and known non-allergens (Dimitrov et al., 2013). ToxinPred considers the presence of certain residues that are generally more dominant in toxins or more dominant in non-toxins and their residue preference at various positions, as well as certain motifs prominent in many toxins. Based on the analysis of datasets of toxic and non-toxic peptides, Cys, His, Asn, and Pro were dominant in toxic peptides, whereas Val, Thr, Arg, Gln, Met, Leu, Lys, Ile, Phe, and Ala were dominant in non-toxic peptides (Gupta et al., 2013).

FlaB was used as the adjuvant for the final vaccine construct. It is the most important component of the flagellar shaft of *V. vulnificus* and has potent mucosal adjuvant activity (Lu et al., 2021). The presence of an adjuvant in a vaccine elicits a heightened immune response. *V. vulnificus* FlaB serves a dual purpose as an adjuvant, as it is both an immune potentiator and a TLR5 agonist (Orosco and Espiritu, 2024), and a mucosal adjuvant that allows the vaccine to be delivered via the mucosal routes and helps it exert its effect under the harsh conditions of mucosal tissues (Freytag and Clements, 2015).

The FlaB adjuvant was linked to the N-terminus using an EAAAK linker, which helped stabilize the construct by limiting its interaction with other regions of the vaccine and allowed for easier separation (Arai et al., 2001). The LBL epitopes were joined by KK linkers, which are the target sequence for cathepsin B, a lysosomal protease important for antigen processing (Ayyagari et al., 2022). The CTL epitopes were joined by AAY linkers as the flanking Ala and Tyr residues enhance CTL epitope presentation by preventing the inhibition of proteasomal digestion (Ayyagari et al., 2022). The HTL epitopes were joined by GPGPG linkers. Regions rich in Gly and Pro are associated with β-turns; therefore, the presence of GPGPG linkers at every 15-20 residues may assist in the formation of secondary and tertiary structures to facilitate antigen expression (Livingston et al., 2002). All linkers effectively separate the epitopes and prevent the inadvertent induction of antibodies from the sequence of two or more epitopes directly joined together, known as junctional epitopes or neoepitopes (Ayyagari et al., 2022). The HEYGAEALERAG linker joining different epitope groups contains five specific cleavage sites for eukaryotic proteasomal degradation for efficient separation

(Dolenc et al., 1998). Finally, the 6x His-tag at the end of the sequence was added for purification of the vaccine construct (Ayyagari et al., 2022).

The final vaccine construct has a molecular weight of approximately 90 kDa. Proteins ≤110 kDa are considered suitable vaccine constructs because of their ease of purification (Barh et al., 2013). A pI of 9.09 indicates that the vaccine construct is alkaline in nature. An aliphatic index within the range of 66.5–84.33 indicates that the vaccine construct is thermally stable. An instability index of <40 indicates that the protein is likely to be stable in vitro. The negative GRAVY score indicates that the protein is hydrophilic and strongly associates with water molecules. The high extinction coefficient, defined as the absorption of light in a medium of a chemical species at a particular wavelength, indicates that the protein may be characterized using spectral UV analysis for downstream studies (Kumar et al., 2023). The 30-hour half-life of the vaccine construct in mammalian reticulocytes in vitro is similar to previously developed vaccine candidates that were found to induce robust humoral and cellular responses in mice (Foroutan et al., 2020). As the vaccine construct does not have homology with any swine proteins, it is non-cross-reactive and will therefore not trigger an autoimmune response upon administration to swine (Umar et al., 2021). Finally, the vaccine construct must be soluble upon overexpression in *E. coli* because insoluble recombinant proteins produced in *E. coli* systems may form insoluble inclusion bodies or become non-functional due to lack of proper folding (Sarkar et al., 2020). Taken together, these physicochemical properties showed that the vaccine construct was safe, stable, and effective. Moreover, the properties reported in this study provide insights into potential methods for characterizing and purifying vaccines during clinical studies.

The secondary and tertiary structures of the final vaccine construct were predicted. The high percentage of alpha helices in the secondary structure indicates that a high number of hydrogen bonds contributing to the stability of the vaccine construct (Alihodžić et al., 2018). On the other hand, the high percentage of random coils contributes to the flexibility of the vaccine construct (Rostaminia et al., 2021). Similarly, globular and disordered regions contribute to the stability and flexibility of the vaccine construct, respectively (Ameri et al., 2022; Shen, 2023).

AlphaFold2 uses deep learning (DL) algorithms to predict tertiary structures of proteins from their amino acid sequences through multiple sequence alignment with homologous sequences and training on data with known protein structures (Yang et al., 2023). In 2020, AlphaFold2 won the CASP14 competition to predict protein structures with the highest accuracy (Yang et al., 2023), cementing it as a highly reliable protein structure prediction program. GalaxyRefine improves protein structures through side-chain rebuilding, side-chain repacking, and overall structural relaxation in a molecular dynamics simulation (Heo et al., 2013). It was the best-performing refinement program in CASP10 in 2012 (Heo et al., 2013) and has since improved. GalaxyRefine returns five (5) refined models with various scores compared to the initial structure. The global distance test (GDT) and RMSD are measures of similarity between two protein structures with the same amino acid sequence. GDT computes the percentage of alpha carbons that are found within a certain cutoff distance of each other (Read and Chavali, 2007), whereas RMSD computes the deviation of the positions of the alpha carbons from their positions in the initial structure (Sargsyan et al., 2017). There are two types of GDT: GDT-TS (total score) and GDT-HA (high accuracy). GDT-HA uses smaller cutoff distances compared to GDT-TS (Read and Chavali, 2007). The MolProbity score is based on the clash score, poor rotamers, and Rama-favored scores. The clash score is the number of clashes per 1000 atoms, poor rotamers are conformations that fall outside the outlier contours of the reference dataset, and the Rama-favored score is the percentage of residues with backbone ϕ, ψ angles, and side-chain rotamer χ angles that fall within the favored regions of the Ramachandran plot (Chen et al., 2010; Hintze et al., 2016). The lower the MolProbity score, the higher the quality of

the predicted structure (Chen et al., 2015). The results of GalaxyRefine showed that the predicted tertiary structure of the vaccine construct was significantly improved.

The z-score is a measure of the deviation of the total energy of the structure from the energy distribution of random conformations, and is indicative of the overall model quality. In ProSA, the z-score of the query structure was plotted against the z-scores of the experimentally derived structures from the PDB. This plot can be used to compare the z-score of the query structure to the z-scores of proteins of similar sizes (Wiederstein and Sippl, 2007). As shown in Figure 3A, the z-score of the vaccine construct was at the high end of the z-scores in its size group. However, there are proteins in the plot that are both larger and smaller with similar and even higher z-scores; therefore, the predicted conformation of the vaccine construct is feasible. The local model quality shows the energy plotted as a function of amino acid sequence position. Positive values correspond to erroneous parts of the model (Wiederstein and Sippl, 2007). The majority of the residues in the energy plot of the vaccine construct had negative values, indicating that most regions of the structure were of sound quality. ERRAT detects regions of protein structures with erroneous atom distributions through comparison with a database of proteins with correct atom distributions (Colovos and Yeates, 1993). In general, a high-resolution structure has an ERRAT score of 95% or higher (Elengoe et al., 2014). The Ramachandran plot in Figure 4 shows the distribution of residues across regions with varying levels of acceptability depending on their backbone ϕ, ψ angles, and side-chain rotamer χ angles. Protein structures with more than 90% of residues in Rama-favored regions are considered accurate (Sumitha et al., 2020).

In the immune simulation, the ASFV+PCV2 vaccine construct and the vaccine construct with PCV2 epitopes alone both had the highest induced T-cell population counts relative to the other groups. Although a slight increase in antibody titers and T-cell population counts was observed after the primary immunization, these along with the B-cell population counts were significantly boosted following the secondary immunization. The results of the immune simulation showed that the epitopes of both ASFV and PCV2 alone are capable of inducing an immune response, and that at least a secondary immunization is required for more robust protection.

The CTL epitopes were docked to SLA-1*04:01, and the final vaccine construct was docked to TLR5. SLA-1*04:01 is commonly found in five different swine breeds (Ho et al., 2009), and has previously been used in molecular docking experiments against CTL epitopes for swine viruses (Zhang et al., 2023; Zhao et al., 2023). TLR5 was chosen as the docking receptor for the final vaccine construct because FlaB and FliC are TLR5 agonists, as TLR5 specifically recognizes flagellins. As no structure of porcine TLR5 is available in PDB, human TLR5 was used. Human TLR5 is 77.8% homologous to porcine TLR5, while the Toll-interleukin-1 receptor (TIR) domain, the key intracellular signaling domain, has 86% homology (Li et al., 2011). TLRs are key regulators of both innate and adaptive immunity. Upon activation, they initiate signaling cascades that result in the upregulation or downregulation of genes to enact events such as inflammatory responses and cytokine production (El-Zayat et al., 2019).

A 200-ns molecular dynamics simulation was performed for the vaccine-TLR5 complex. The stabilization of the RMSD indicates that the vaccine and TLR5 were able to form a stable complex. As the LBL epitopes form a random coil opposite the docked end of the vaccine, high RMSF fluctuations within this range are expected and are likely to have contributed the most to RMSD enhancement. The lower fluctuations before and after the LBL epitopes are from the FlaB adjuvant and CTL epitopes, which make up the majority of the interface interacting with TLR5, respectively. Both components are mainly composed of alpha helices, which contribute to their stability and low fluctuations. The overall decrease in the Rg of the complex indicates an increase in the compactness of the complex, contributing

to its stability. The overall increase in the number of hydrogen bonds formed between the vaccine and TLR5 showed an increase in the stability at the interacting interface of the complex. The decrease in the SASA value indicates that over time, fewer molecules are exposed to the solvent, and more become buried within the protein complex, indicating an increase in the interaction between components of the complex (Jyotisha et al., 2022; Rajput et al., 2022). Overall, MD analysis showed that the vaccine-TLR5 complex stabilized over time, indicating successful binding of the vaccine to TLR5.

It is worth noting that while ASFV and PCV2 are well-characterized and well-documented, their mechanism of co-infection and interaction within the host still requires further probing. The induction of other cytokines that could potentially alleviate or aggravate pathogenesis can only be confirmed through in vitro experiments. Furthermore, the limitations of current protein structure prediction may result in loops of unknown regions that consequently affect docking and dynamics predictions. The vaccine construct in this study has been designed to be as feasible and as effective as possible based on the predicted parameters; nevertheless, the synthesis and experimentation of the vaccine in the laboratory and in clinical trials must be performed in order to ultimately confirm the computational findings. However, while in silico methods alone are not sufficient in vaccine design, they are useful in performing an initial screening for selecting the best components and configurations among a vast number of potential epitopes and adjuvants and provide a foundation upon which a final vaccine can be created. Moreover, in silico methods are continuously evolving, and reverse vaccinology and immunoinformatics approaches will only improve moving forward.

CONCLUSIONS

In this study, a multi-epitope, multivalent subunit vaccine against co-infecting ASFV and PCV2 was computationally designed using LBL, CTL, and HTL epitopes screened from 100 ASFV proteomes and the Cap, Rep, and ORF3 proteins of PCV2. The screened epitopes were predicted to be antigenic, non-allergenic, non-toxic, and immunogenic. Likewise, the final vaccine construct adjuvanted with *V. vulnificus* FlaB was predicted to be antigenic, non-allergenic, non-toxic, and stable. Immune simulations revealed that the vaccine would be capable of eliciting humoral, T-cell, and B-cell responses that are more robust than the vaccine with ASFV or PCV2 epitopes alone, adjuvant alone, and a previously designed vaccine against ASFV. Molecular docking of the PCV2 CTL epitopes to SLA-1*04:01 and the vaccine construct to TLR5 was successful, as indicated by the highly negative binding energies and substantial number of molecular interactions. Finally, a molecular dynamics simulation of the vaccine-TLR5 complex showed that the complex stabilized over time, as measured by RMSD, RMSF, Rg, SASA, and the number of formed hydrogen bonds. Further cell-based in vitro assays and in vivo challenge trials in swine are required to validate the efficacy of the designed vaccine. The interaction between co-infecting ASFV and PCV2 within the host, especially regarding the effects of IL-10 in the presence of PCV2 infection, must be further explored to improve the current design. This study serves as a step toward the eradication of ASFV and PCV2, and the improvement of food security worldwide and is the first study to design a multi-epitope multivalent subunit vaccine against ASFV and PCV2.

ACKNOWLEDGEMENTS

The authors would like to thank the Philippine Council for Agriculture, Aquatic and Natural Resources Research and Development (PCAARRD), who funded the project under the Virology and Vaccine Research Program. The authors

would also like to thank the Department of Science and Technology - S&T Fellows Program, the Department of Science and Technology - Science Education Institute (DOST-SEI) Career Incentive Program, the Department of Science and Technology - Industrial Technology Development Institute (DOST-ITDI), and the Department of Science and Technology – Advanced Science and Technology Institute (DOST-ASTI) Computing and Archiving Research Environment (COARE) for their support to this research. The authors would also like to thank Dr. Mark Andrian B. Macalalad for his valuable insights concerning the molecular dynamics section of the study.

AUTHOR CONTRIBUTIONS

Lauren Emily Fajardo: Methodology; Formal analysis; Investigation; Writing – original draft preparation; Writing – review and editing.
Edward C. Banico: Methodology; Formal analysis; Investigation; Writing – review and editing.
Ella Mae Joy S. Sira: Methodology; Formal analysis; Investigation; Writing – review and editing.
Nyzar Mabeth O. Odchimar: Methodology; Formal analysis; Investigation.
Fredmoore L. Orosco: Conceptualization; Funding acquisition; Supervision; Writing – review and editing.

CONFLICT OF INTEREST

All authors declare that they have no competing interests.

REFERENCES

Abraham, M.J., Murtola, T., Schulz, R., Páll, S., Smith, J.C., Hess, B., Lindahl, E., 2015. GROMACS: High performance molecular simulations through multi-level parallelism from laptops to supercomputers. SoftwareX. 1-2, 19–25.

Alihodžić, S., Bukvić, M., Elenkov, I.J., Hutinec, A., Koštrun, S., Pešić, D., Saxty, G., Tomašković, L., Žiher, D., 2018. Current trends in macrocyclic drug discovery and beyond-Ro5. In: Witty, J.E., Cox, B. (Eds.), Progress in medicinal chemistry. Elsevier, Amsterdam, pp. 113–233.

Althwaiqeb, S.A., Fakoya, A.O., Bordoni, B., 2023. Histology, B Cell Lymphocyte. Available online: https://www.ncbi.nlm.nih.gov/books/NBK560905/

Altschul, S.F., Gish, W., Miller, W., Myers, E.W., Lipman, D.J., 1990. Basic local alignment search tool. J. Mol. Biol. 215(3), 403–410.

Ameri, M., Nezafat, N., Eskandari, S., 2022. The potential of intrinsically disordered regions in vaccine development. Expert. Rev. Vaccines. 21(1), 1–3.

Arai, R., Ueda, H., Kitayama, A., Kamiya, N., Nagamune, T., 2001. Design of the linkers which effectively separate domains of a bifunctional fusion protein. Protein Eng. Des. Sel. 14(8), 529–532.

Arzt, J., White, W.R., Thomsen, B. V., Brown, C.C., 2010. Agricultural diseases on the move early in the third millennium. Vet. Pathol. 47(1), 15–27.

Ayyagari, V.S., Venkateswarulu T.C., Karlapudi, A.P., Srirama, K., 2022. Design of a multi-epitope-based vaccine targeting M-protein of SARS-CoV2: an immunoinformatics approach. J. Biomol. Struct. Dyn. 40(7), 2963–2977.

Barh, D., Barve, N., Gupta, K., Chandra, S., Jain, N., Tiwari, S., Leon-Sicairos, N., Canizalez-Roman, A., Rodrigues dos Santos, A., Hassan, S.S., Almeida, S., Thiago Jucá Ramos, R., Augusto Carvalho de Abreu, V., Ribeiro Carneiro, A., de Castro Soares, S., Luiz de Paula Castro, T., Miyoshi, A., Silva, A., Kumar, A., Narayan Misra, A., Blum, K., Braverman, E.R., Azevedo, V., 2013. Exoproteome and secretome derived broad spectrum novel drug and vaccine

candidates in Vibrio cholerae targeted by Piper betel derived compounds. PLoS One. 8(1), e52773.
Berman, H.M., Westbrook, J., Feng, Z., Gilliland, G., Bhat, T.N., Weissig, H., Shindyalov, I.N., Bourne, P.E., 2000. The protein data bank. Nucleic. Acids. Res. 28(1), 235–242.
Blum, J.S., Wearsch, P.A., Cresswell, P., 2013. Pathways of antigen processing. Annu. Rev. Immunol. 31(1), 443–473.
Buan, A.K.G., Reyes, N.A.L., Pineda, R.N.B., Medina, P.M.B., 2022. In silico design and evaluation of a multi-epitope and multi-antigenic African swine fever vaccine. ImmunoInformatics. 8, 100019.
Buragohain, L., Barman, N.N., Sen, S., Bharali, A., Dutta, B., Choudhury, B., Suresh, K.P., Gaurav, S., Kumar, R., Ali, S., Kumar, S., Singh Malik, Y., 2023. Transmission of African swine fever virus to the wild boars of Northeast India. Vet. Q. 43(1), 1–10.
Calis, J.J.A., Maybeno, M., Greenbaum, J.A., Weiskopf, D., De Silva, A.D., Sette, A., Keşmir, C., Peters, B., 2013. Properties of MHC class I presented peptides that enhance immunogenicity. PLoS. Comput. Biol. 9(10), e1003266.
Chen, S., Li, X., Zhang, L., Zheng, J., Yang, L., Niu, G., Zhang, H., Ren, Y., Qian, J., Sun, C., Ren, L., 2023. Phylogenetic and structural analysis of porcine circovirus type 2 from 2016 to 2021 in Jilin Province, China. Microorganisms. 11(4), 983.
Chen, V.B., Arendall, W.B., Headd, J.J., Keedy, D.A., Immormino, R.M., Kapral, G.J., Murray, L.W., Richardson, J.S., Richardson, D.C., 2010. MolProbity: all-atom structure validation for macromolecular crystallography. Acta. Crystallogr. D. Biol. Crystallogr. 66(1), 12–21.
Chen, V.B., Wedell, J.R., Wenger, R.K., Ulrich, E.L., Markley, J.L., 2015. MolProbity for the masses–of data. J. Biomol. NMR. 63, 77–83.
Clark, D.P., Pazdernik, N.J., 2016. Immune technology. In: Clark, D.P., Pazdernik, N.J. (Eds.), Biotechnology, Elsevier, London, pp. 181–217.
Clifford, J.N., Høie, M.H., Deleuran, S., Peters, B., Nielsen, M., Marcatili, P., 2022. BepiPred-3.0: Improved B-cell epitope prediction using protein language models. Protein. Sci. 31(12), e4497.
Colovos, C., Yeates, T.O., 1993. Verification of protein structures: Patterns of nonbonded atomic interactions. Protein. Sci. 2(9), 1511–1519.
Darwich, L., Balasch, M., Plana-Durán, J., Segalés, J., Domingo, M., Mateu, E., 2003. Cytokine profiles of peripheral blood mononuclear cells from pigs with postweaning multisystemic wasting syndrome in response to mitogen, superantigen or recall viral antigens. J. Gen. Virol. 84(12), 3453–3457.
Darwich, L., Segalés, J., Resendes, A., Balasch, M., Plana-Durán, J., Mateu, E., 2008. Transient correlation between viremia levels and IL-10 expression in pigs subclinically infected with porcine circovirus type 2 (PCV2). Res. Vet. Sci. 84(2), 194–198.
dela Cruz, A., Palmieri, C., Azul, R., Legaspi, C., Lola, S., Barnes, T.S., Parke, C.R., Turni, C., Alawneh, J.I., Baluyut, A.S., Basinang, V.G., David, J.E., de Castro, R.O., Domingo, R., Francisco, E., Ignacio, C., Lapuz, E.L., Mananggit, M.R., Retes, L., Villar, E.C., Blackall, P.J., Meers, J., 2021. Detection of porcine circovirus type 2 (PCV2) in the Philippines and the complexity of PCV2-associated disease diagnosis. Trop. Anim. Health. Prod. 53(3), 371.
Desta, I.T., Porter, K.A., Xia, B., Kozakov, D., Vajda, S., 2020. Performance and its limits in rigid body protein-protein docking. Structure. 28(9), 1071-1081.
Dhanda, S.K., Karosiene, E., Edwards, L., Grifoni, A., Paul, S., Andreatta, M., Weiskopf, D., Sidney, J., Nielsen, M., Peters, B., Sette, A., 2018. Predicting HLA CD4 immunogenicity in human populations. Front. Immunol. 9, 1369.
Díez-Rivero, C.M., Reche, P., 2009. Discovery of conserved epitopes through sequence variability analyses. In: Flower, D.R., Davies, M., Ranganathan, S. (Eds.), Bioinformatics for immunomics. Springer, New York, pp. 95–101.

Dimitrov, I., Flower, D.R., Doytchinova, I., 2013. AllerTOP - a server for in silico prediction of allergens. BMC Bioinformatics. 14, 1-9.
Dolenc, I., Seemüller, E., Baumeister, W., 1998. Decelerated degradation of short peptides by the 20S proteasome. FEBS Lett. 434(3), 357–361.
Doytchinova, I.A., Flower, D.R., 2007. VaxiJen: a server for prediction of protective antigens, tumour antigens and subunit vaccines. BMC Bioinformatics. 8, 1-7.
Du, Q., Zhang, H., He, M., Zhao, X., He, J., Cui, B., Yang, X., Tong, D., Huang, Y., 2019. Interleukin-10 promotes porcine circovirus type 2 persistent infection in mice and aggravates the tissue lesions by duppression of T vell infiltration. Front. Microbiol. 10, 2050.
Dundon, W.G., Franzo, G., Settypalli, T.B.K., Dharmayanti, N.L.P.I., Ankhanbaatar, U., Sendow, I., Ratnawati, A., Sainnokhoi, T., Molini, U., Cattoli, G., Lamien, C.E., 2022. Evidence of coinfection of pigs with African swine fever virus and porcine circovirus 2. Arch. Virol. 167, 207–211.
Elengoe, A., Naser, M., Hamdan, S., 2014. Modeling and docking studies on novel mutants (K71L and T204V) of the ATPase domain of human heat shock 70 kDa protein 1. Int. J. Mol. Sci. 15(4), 6797–6814.
El-Zayat, S.R., Sibaii, H., Mannaa, F.A., 2019. Toll-like receptors activation, signaling, and targeting: an overview. Bull. Natl. Res. Cent. 43(1), 187.
Fagbohun, O.A., Aiki-Raji, C.O., Omotosho, O.O., 2022. Contriving a multi-epitope vaccine against African swine fever utilizing immunoinformatics. Available online: https://www.researchsquare.com/article/rs-1978238/v1.
Food and Agriculture Organization of the United Nations, 2024. African swine fever (ASF) situation update in Asia & Pacific. Available online: https://www.fao.org/animal-health/situation-updates/asf-in-asia-pacific/en.
Foroutan, M., Ghaffarifar, F., Sharifi, Z., Dalimi, A., 2020. Vaccination with a novel multi-epitope ROP8 DNA vaccine against acute Toxoplasma gondii infection induces strong B and T cell responses in mice. Comp. Immunol. Microbiol. Infect. Dis. 69, 101413.
Freytag, L.C., Clements, J.D., 2015. Mucosal adjuvants: New developments and challeneges. In: Mestecky, J., Strober, W., Russell, M.W., Kelsall, B.L. Cheroutre, H., Lambrecht, B.N. (Eds.), Mucosal Immunology, Elsevier, London, pp. 1183–1199.
Garnier, J., Gibrat, J.F., Robson, B., 1996. GOR method for predicting protein secondary structure from amino acid sequence. In: Doolittle, R.F. (Ed.), Computer methods or macromolecular sequence analysis, Elsevier, London, pp. 540–553.
Gasteiger, E., Hoogland, C., Gattiker, A., Duvaud, S., Wilkins, M.R., Appel, R.D., Bairoch, A., 2005. Protein identification and analysis tools on the ExPASy server. In: Walker, J.M. (Ed.), The proteomics protocols handbook. Humana, Totowa, New Jersey, pp. 571–607.
Guo, J., Hou, L., Zhou, J., Wang, D., Cui, Y., Feng, X., Liu, J., 2022. Porcine circovirus type 2 vaccines: commercial application and research advances. Viruses. 14(9), 2005.
Gupta, S., Kapoor, P., Chaudhary, K., Gautam, A., Kumar, R., Raghava, G.P.S., 2013. In silico approach for predicting toxicity of peptides and proteins. PLoS One. 8(9), e73957.
Haste Andersen, P., Nielsen, M., Lund, O., 2006. Prediction of residues in discontinuous B-cell epitopes using protein 3D structures. Protein. Sci. 15(11), 2558–2567.
Heo, L., Park, H., Seok, C., 2013. GalaxyRefine: protein structure refinement driven by side-chain repacking. Nucleic. Acids. Res. 41(W1), W384–W388.
Herrera, L.R.D.M., Bisa, E.P., 2021. In silico analysis of highly conserved cytotoxic T-cell epitopes in the structural proteins of African swine fever virus. Vet. World. 14(10), 2625–2633.

Hintze, B.J., Lewis, S.M., Richardson, J.S., Richardson, D.C., 2016. Molprobity's ultimate rotamer-library distributions for model validation. Proteins: Structure, Function, and Bioinformatics. 84(9), 1177–1189.

Ho, C.S., Lunney, J.K., Ando, A., Rogel-Gaillard, C., Lee, J.H., Schook, L.B., Smith, D.M., 2009. Nomenclature for factors of the SLA system, update 2008. Tissue Antigens. 73(4), 307–315.

Honorato, R.V., Koukos, P.I., Jiménez-García, B., Tsaregorodtsev, A., Verlato, M., Giachetti, A., Rosato, A., Bonvin, A.M.J.J., 2021. Structural biology in the clouds: the WeNMR-EOSC Ecosystem. Front. Mol. Biosci. 8, 729513.

Hsu, C.H., Montenegro, M., Perez, A., 2023. Space–time dynamics of African swine fever spread in the Philippines. Microorganisms. 11(6), 1492.

Juan, A.A., Palma, K.C., Suarez, M., Herrera-Ong, L.D.M., 2022. Immunoinformatics-based identification of highly conserved cytotoxic T-cell epitopes in polyprotein pp220 of African swine fever virus. Biomed. Biotechnol. Res. J. 6(3), 319-325.

Jumper, J., Evans, R., Pritzel, A., Green, T., Figurnov, M., Ronneberger, O., Tunyasuvunakool, K., Bates, R., Žídek, A., Potapenko, A., Bridgland, A., Meyer, C., Kohl, S.A.A., Ballard, A.J., Cowie, A., Romera-Paredes, B., Nikolov, S., Jain, R., Adler, J., Back, T., Petersen, S., Reiman, D., Clancy, E., Zielinski, M., Steinegger, M., Pacholska, M., Berghammer, T., Bodenstein, S., Silver, D., Vinyals, O., Senior, A.W., Kavukcuoglu, K., Kohli, P., Hassabis, D., 2021. Highly accurate protein structure prediction with AlphaFold. Nature. 596(7873), 583–589.

Jyotisha, Singh, S., Qureshi, I.A., 2022. Multi-epitope vaccine against SARS-CoV-2 applying immunoinformatics and molecular dynamics simulation approaches. J. Biomol. Struct. Dyn. 40(7), 2917–2933.

Karosiene, E., Lundegaard, C., Lund, O., Nielsen, M., 2012. NetMHCcons: a consensus method for the major histocompatibility complex class I predictions. Immunogenetics. 64, 177–186.

Kim, G., Park, J.E., Kim, S.J., Kim, Y., Kim, W., Kim, Y.K., Jheong, W., 2023. Complete genome analysis of the African swine fever virus isolated from a wild boar responsible for the first viral outbreak in Korea, 2019. Front. Vet. Sci. 9, 1080397.

Kozakov, D., Beglov, D., Bohnuud, T., Mottarella, S.E., Xia, B., Hall, D.R., Vajda, S., 2013. How good is automated protein docking? Proteins: Structure, Function, and Bioinformatics. 81(12), 2159–2166.

Kozakov, D., Hall, D.R., Xia, B., Porter, K.A., Padhorny, D., Yueh, C., Beglov, D., Vajda, S., 2017. The ClusPro web server for protein–protein docking. Nat. Protoc. 12(2), 255–278.

Kumar, K.M., Karthik, Y., Ramakrishna, D., Balaji, S., Skariyachan, S., Murthy, T.P.K., Sakthivel, K.M., Alotaibi, B.S., Shukry, M., Sayed, S.M., Mushtaq, M., 2023. Immunoinformatic exploration of a multi-epitope-based peptide vaccine candidate targeting emerging variants of SARS-CoV-2. Front. Microbiol. 14, 1251716.

Laskowski, R.A., Jabłońska, J., Pravda, L., Vařeková, R.S., Thornton, J.M., 2018. PDBsum: Structural summaries of PDB entries. Protein. Sci. 27(1), 129–134.

Laskowski, R.A., MacArthur, M.W., Moss, D.S., Thornton, J.M., 1993. PROCHECK: a program to check the stereochemical quality of protein structures. J. Appl. Crystallogr. 26(2), 283–291.

Lee, H., Heo, L., Lee, M.S., Seok, C., 2015. GalaxyPepDock: a protein–peptide docking tool based on interaction similarity and energy optimization. Nucleic. Acids. Res. 43(W1), W431–W435.

Lei, Y., Shao, J., Ma, F., Lei, C., Chang, H., Zhang, Y., 2020. Enhanced efficacy of a multi-epitope vaccine for type A and O foot-and-mouth disease virus by fusing multiple epitopes with Mycobacterium tuberculosis heparin-binding hemagglutinin (HBHA), a novel TLR4 agonist. Mol. Immunol. 121, 118–126.

Li, H.T., Liu, D., Yang, X.Q., 2011. Identification and functional analysis of a novel single nucleotide polymorphism (SNP) in the porcine Toll like receptor (TLR) 5 gene. Acta. Agric. Scand. A Anim. Sci. 61(4), 161–167.

Linding, R., Russell, R.B., Neduva, V., Gibson, T.J., 2003. GlobPlot: exploring protein sequences for globularity and disorder. Nucleic. Acids. Res. 31(13), 3701–3708.

Liu, H., Zou, J., Liu, R., Chen, J., Li, X., Zheng, H., Li, L., Zhou, B., 2023. Development of a TaqMan-probe-based multiplex real-time PCR for the simultaneous detection of African swine fever virus, porcine circovirus 2, and pseudorabies virus in East China from 2020 to 2022. Vet. Sci. 10(2), 106.

Liu, X., Liu, Y., Zhang, Y., Zhang, F., Du, E., 2020. Incorporation of a truncated form of flagellin (TFlg) into porcine circovirus type 2 virus-like particles enhances immune responses in mice. BMC Vet. Res. 16, 45.

Livingston, B., Crimi, C., Newman, M., Higashimoto, Y., Appella, E., Sidney, J., Sette, A., 2002. A rational strategy to design multiepitope immunogens based on multiple Th lymphocyte epitopes. J. Immun. 168(11), 5499–5506.

Lu, H., Zhou, X., Wu, Z., Zhang, X., Zhu, L., Guo, X., Zhang, Q., Zhu, S., Zhu, H., Sun, H., 2021. Comparison of the mucosal adjuvanticities of two Toll-like receptor ligands for recombinant adenovirus-delivered African swine fever virus fusion antigens. Vet. Immunol. Immunopathol. 239, 110307.

Lu, P., Zhou, J., Wei, S., Takada, K., Masutani, H., Okuda, S., Okamoto, K., Suzuki, M., Kitamura, T., Masujin, K., Kokuho, T., Itoh, H., Nagata, K., 2023. Comparative genomic and transcriptomic analyses of African swine fever virus strains. Comput. Struct. Biotechnol. J. 21, 4322–4335.

Luka, P.D., Adedeji, A.J., Jambol, A.R., Ifende, I. V., Luka, H.G., Choji, N.D., Weka, R., Settypalli, T.B.K., Achenbach, J.E., Cattoli, G., Lamien, C.E., Molini, U., Franzo, G., Dundon, W.G., 2022. Coinfections of African swine fever virus, porcine circovirus 2 and 3, and porcine parvovirus 1 in swine in Nigeria. Arch. Virol. 167(12), 2715–2722.

Magnan, C.N., Randall, A., Baldi, P., 2009. SOLpro: accurate sequence-based prediction of protein solubility. Bioinformatics. 25(17), 2200–2207.

Maki-Yonekura, S., Yonekura, K., Namba, K., 2009. L-type straight flagellar filament made of full-length flagellin. Available online: https://pdbj.org/mine/summary/3a5x.

Maki-Yonekura, S., Yonekura, K., Namba, K., 2010. Conformational change of flagellin for polymorphic supercoiling of the flagellar filament. Nat. Struct. Mol. Biol. 17(4), 417–422.

Maldonado, J., Ségales, J., Calsamiglia, M., Llopart, D., Sibila, M., Lapus, Z., Riera, P., Artigas, C., 2004. Postweaning multisystemic wasting syndrome (PMWS) in the Philippines: Porcine circovirus type 2 (PCV2) detection and characterization. J. Vet. Med. Sci. 66(5), 533–537.

Maleki, A., Russo, G., Parasiliti Palumbo, G.A., Pappalardo, F., 2022. In silico design of recombinant multi-epitope vaccine against influenza A virus. BMC Bioinformatics. 22, 617.

Meng, X.J., 2013. Porcine circovirus type 2 (PCV2): pathogenesis and interaction with the immune system. Annu. Rev. Anim. Biosci. 1(1), 43–64.

Mirdita, M., Schütze, K., Moriwaki, Y., Heo, L., Ovchinnikov, S., Steinegger, M., 2022. ColabFold: making protein folding accessible to all. Nat. Methods. 19(6), 679–682.

Mishra, S., 2020. Designing of cytotoxic and helper T cell epitope map provides insights into the highly contagious nature of the pandemic novel coronavirus SARS-CoV-2. R. Soc. Open. Sci. 7(9), 201141.

Modis, Y., Zhou, K., Kanai, R., Lee, P., Wang, H.W., 2011. Homology model of human Toll-like receptor 5 fitted into an electron microscopy single particle reconstruction. Available online: https://www.rcsb.org/structure/3j0a.

Nagpal, G., Usmani, S.S., Dhanda, S.K., Kaur, H., Singh, S., Sharma, M., Raghava, G.P.S., 2017. Computer-aided designing of immunosuppressive peptides based on IL-10 inducing potential. Sci. Rep. 7, 42851.

Orosco, F.L., Espiritu, L.M., 2024. Navigating the landscape of adjuvants for subunit vaccines: recent advances and future perspectives. Int. J. Appl. Pharmaceut. 10, 18–32.

Ouyang, T., Zhang, X., Liu, X., Ren, L., 2019. Co-infection of swine with porcine circovirus type 2 and other swine viruses. Viruses. 11(2), 185.

Pang, M., Tu, T., Wang, Y., Zhang, P., Ren, M., Yao, X., Luo, Y., Yang, Z., 2022. Design of a multi-epitope vaccine against Haemophilus parasuis based on pan-genome and immunoinformatics approaches. Front. Vet. Sci. 9, 1053198.

Rajput, V.S., Sharma, R., Kumari, A., Vyas, N., Prajapati, V., Grover, A., 2022. Engineering a multi epitope vaccine against SARS-CoV-2 by exploiting its non structural and structural proteins. J. Biomol. Struct. Dyn. 40(19), 9096–9113.

Rapin, N., Lund, O., Bernaschi, M., Castiglione, F., 2010. Computational immunology meets bioinformatics: the use of prediction tools for molecular binding in the simulation of the immune system. PLoS One. 5(4), e9862.

Read, R.J., Chavali, G., 2007. Assessment of CASP7 predictions in the high accuracy template-based modeling category. Proteins. 69(S8), 27–37.

Reynisson, B., Alvarez, B., Paul, S., Peters, B., Nielsen, M., 2020. NetMHCpan-4.1 and NetMHCIIpan-4.0: improved predictions of MHC antigen presentation by concurrent motif deconvolution and integration of MS MHC eluted ligand data. Nucleic. Acids. Res. 48(W1), W449–W454.

Ros-Lucas, A., Correa-Fiz, F., Bosch-Camós, L., Rodriguez, F., Alonso-Padilla, J., 2020. Computational analysis of african swine fever virus protein space for the design of an epitope-based vaccine ensemble. Pathogens. 9(12), 1078.

Rostaminia, S., Aghaei, S.S., Farahmand, B., Nazari, R., Ghaemi, A., 2021. Computational design and analysis of a multi-epitope against influenza A virus. Int. J. Pept. Res. Ther. 27, 2625–2638.

Rowaiye, A.B., Oli, A.N., Asala, M.T., Nwonu, E.J., Njoku, M.O., Asala, O.O., Salami, S.A., Mbachu, N.A., 2023. Design of multiepitope vaccine candidate from a major capsid protein of the African swine fever virus. Vet. Vaccine. 2(1), 100013.

Saha, S., Raghava, G.P.S., 2006. Prediction of continuous B-cell epitopes in an antigen using recurrent neural network. Proteins. 65(1), 40–48.

Saha, S., Raghava, G.P.S., 2007. Prediction methods for B-cell epitopes. In: Flower, D.R. (Ed.), Immunoinformatics: predicting immunogenicity in silico. Humana, Totowa, New Jersey, pp. 387–394.

Šali, A., Blundell, T.L., 1993. Comparative protein modelling by satisfaction of spatial restraints. J. Mol. Biol. 234(3), 779–815

Sargsyan, K., Grauffel, C., Lim, C., 2017. How molecular size impacts RMSD applications in molecular dynamics simulations. J. Chem. Theory. Comput. 13(4), 1518–1524.

Sarkar, B., Ullah, M.A., Araf, Y., Rahman, M.S., 2020. Engineering a novel subunit vaccine against SARS-CoV-2 by exploring immunoinformatics approach. Inform. Med. Unlocked. 21, 100478.

Savar, N., Bouzari, S., 2014. In silico study of ligand binding site of toll-like receptor 5. Adv. Biomed. Res. 3(1), 41.

Sayers, E.W., Bolton, E.E., Brister, J.R., Canese, K., Chan, J., Comeau, D.C., Connor, R., Funk, K., Kelly, C., Kim, S., Madej, T., Marchler-Bauer, A., Lanczycki, C., Lathrop, S., Lu, Z., Thibaud-Nissen, F., Murphy, T., Phan, L., Skripchenko, Y., Tse, T., Wang, J., Williams, R., Trawick, B.W., Pruitt, K.D., Sherry, S.T., 2022. Database resources of the national center for biotechnology information. Nucleic. Acids. Res. 50(D1), D20–D26.

Schrödinger, 2023. PyMOL v2.5.5 (Version 2.5.5). Available online: https://pymol.org/.

Shen, C.H., 2023. Diagnostic molecular biology, (2nd edition). Elsevier, London.
Simbulan, A.M., Banico, E.C., Sira, E.M.J.S., Odchimar, N.M.O., Orosco, F.L., 2024. Immunoinformatics-guided approach for designing a pan-proteome multi-epitope subunit vaccine against African swine fever virus. Sci. Rep. 14, 1354.
Singh, H., Ansari, H.R., Raghava, G.P.S., 2013. Improved method for linear B-cell epitope prediction using antigen's primary sequence. PLoS One. 8, e62216.
Singh, H., Gupta, S., Gautam, A., Raghava, G.P.S., 2015. Designing B-cell epitopes for immunotherapy and subunit vaccines. In: Houen, G. (Ed.), Peptide antibodies: methods and protocols. Humana, New York, pp. 327–340.
Sippl, M.J., 1993. Recognition of errors in three-dimensional structures of proteins. Proteins. 17(4), 355–362.
Sira, E.M.J.S., Banico, E.C., Fajardo, L.E., Odchimar, N.M., Simbulan, A.M., Orosco, F.L., 2025. Current strategies, advances, and challenges in multi-epitope subunit vaccine development for African swine fever virus. Vet. Integ. Sci. 23(1), 1–48.
Stranzl, T., Larsen, M.V., Lundegaard, C., Nielsen, M., 2010. NetCTLpan: pan-specific MHC class I pathway epitope predictions. Immunogenetics. 62, 357–368.
Sumitha, A., Devi, P.B., Hari, S., Dhanasekaran, R., 2020. Covid-19 - In silico structure prediction and molecular docking studies with doxycycline and quinine. Biomed. pharmacol. J. 13(3), 1185–1193.
Tamura, K., Stecher, G., Kumar, S., 2021. MEGA11: molecular evolutionary genetics analysis version 11. Mol. Biol. Evol. 38(7), 3022–3027.
Tarrahimofrad, H., Rahimnahal, S., Zamani, J., Jahangirian, E., Aminzadeh, S., 2021. Designing a multi-epitope vaccine to provoke the robust immune response against influenza A H7N9. Sci. Rep. 11, 24485.
Umar, A., Haque, A., Alghamdi, Y.S., Mashraqi, M.M., Rehman, A., Shahid, F., Khurshid, M., Ashfaq, U.A., 2021. Development of a candidate multi-epitope subunit vaccine against Klebsiella aerogenes: subtractive proteomics and immuno-informatics approach. Vaccines (Basel). 9(11), 1373.
Vajda, S., Yueh, C., Beglov, D., Bohnuud, T., Mottarella, S.E., Xia, B., Hall, D.R., Kozakov, D., 2017. New additions to the ClusPro server motivated by CAPRI. Proteins. 85(3), 435–444.
Vangone, A., Bonvin, A.M., 2015. Contacts-based prediction of binding affinity in protein–protein complexes. Elife. 4, e07454.
Wiederstein, M., Sippl, M.J., 2007. ProSA-web: interactive web service for the recognition of errors in three-dimensional structures of proteins. Nucleic. Acids. Res. 35, W407–W410.
World Organisation for Animal Health, 2024. African swine fever (ASF) – situation report 53. Available online: https://www.woah.org/app/uploads/2024/06/asf-report53.pdf.
Xue, L.C., Rodrigues, J.P., Kastritis, P.L., Bonvin, A.M., Vangone, A., 2016. PRODIGY: a web server for predicting the binding affinity of protein–protein complexes. Bioinformatics. 32(23), 3676–3678.
Yadav, D.K., Yadav, N., Khurana, S.M.P., 2020. Vaccines: present status and applications. In: Verma, A.S., Singh, A. (Eds.), Animal biotechnology: models in discovery and translation. Elsevier, London, pp. 523–542.
Yang, Z., Zeng, X., Zhao, Y., Chen, R., 2023. AlphaFold2 and its applications in the fields of biology and medicine. Signal Transduct. Target. Ther. 8, 115.
Yao, B., Zhang, L., Liang, S., Zhang, C., 2012. SVMTriP: A method to predict antigenic epitopes using support vector machine to integrate tri-peptide similarity and propensity. PLoS One. 7(9), e45152.
Zajonc, D.M., 2020. Unconventional peptide presentation by classical MHC class i and implications for T and NK cell activation. Int. J. Mol. Sci. 21(20), 7561.

Zhang, G., Liu, W., Yang, S., Song, S., Ma, Y., Zhou, G., Liang, X., Miao, C., Li, J., Liu, Y., Shao, J., Chang, H., 2023. Evaluation of humoral and cellular immune responses induced by a cocktail of recombinant African swine fever virus antigens fused with OprI in domestic pigs. Virol. J. 20, 104.

Zhang, J.M., An, J., 2007. Cytokines, inflammation, and pain. Int. Anesthesiol. Clin. 45(2), 27–37.

Zhang, N., Qi, J., Feng, S., Gao, F., Liu, J., Pan, X., Chen, R., Li, Q., Chen, Z., Li, X., Xia, C., Gao, G.F., 2011a. Crystal structure of swine major histocompatibility complex class I SLA-1*0401 and identification of 2009 pandemic swine-origin influenza A H1N1 virus cytotoxic T lymphocyte epitope peptides. J. Virol. 85(22), 11709–11724.

Zhang, X., Guan, X., Wang, Q., Wang, X., Yang, X., Li, S., Zhao, X.T., Yuan, M., Liu, X., Qiu, H.J., Li, Y., 2023. Identification of the p34 protein of African swine fever virus as a novel viral antigen with protection potential. Viruses. 16(1), 38.

Zhao, X., Wang, X., Yuan, M., Zhang, X., Yang, X., Guan, X., Li, S., Ma, J., Qiu, H.-J., Li, Y., 2023. Identification of two novel T cell epitopes on the E2 protein of classical swine fever virus C-strain. Vet. Microbiol. 284, 109814.

Zhou, K., Kanai, R., Lee, P., Wang, H.-W., Modis, Y., 2012. Toll-like receptor 5 forms asymmetric dimers in the absence of flagellin. J. Struct. Biol. 177(2), 402–409.

How to cite this article;

Lauren Emily Fajardo, Edward C. Banico, Ella Mae Joy S. Sira, Nyzar Mabeth O. Odchimar and Fredmoore L. Orosco. Computational multi-epitope based design of a multivalent subunit vaccine against co-infecting African swine fever virus and porcine circovirus type 2. Veterinary Integrative Sciences. 2025; 23(3): e2025065-1-30.